Investigating upstream open reading frame-related mechanisms for protein upregulation of brain-derived neurotrophic factor (BDNF)



Thomas Goedert

St Hugh's College, University of Oxford

Thesis submitted for the degree of

MSc by Research in Paediatrics

Acknowledgements

I would like to thank Professor Matthew Wood for giving me the opportunity to work in his group, and to develop as a scientist. A huge thanks goes to Dr Thomas Roberts for all his support throughout my time in the lab, I have learnt a lot from you and have really enjoyed our discussions.

A big thanks must also go to Dr Britt Hanson and Dr Rushdie Abuhamdah who gave up their time to teach and support me in the lab. Rushdie, I will particularly miss our stimulating chats and your exquisite coffee.

Finally, I would also like to thank the whole of the Wood group for being so welcoming and supportive. I have learnt a lot this year and enjoyed every moment of it.

Table of Contents

Abstract 1

1 Introduction 2

1.1 Upstream open reading frames (uORFs) 2
1.1.1 uORFs and the ribosome 2
1.1.2 Modulatory roles of uORFs 5
1.1.3 uORFs in disease 6

1.2 Brain-derived neurotrophic factor (BDNF) 7
1.2.1 BDNF gene (*BDNF*) 7
1.2.2 BDNF synthesis and function 8
1.2.3 Current approaches for upregulating BDNF protein levels 9

1.3 Antisense oligonucleotides (ASOs) 10
1.3.1 ASO-mediated exon skipping 10
1.3.2 Targeting of ASOs 14
1.3.2.1 ASO backbone chemical modifications 14
1.3.2.2 ASO ribose sugar chemical modifications 15
1.3.3 ASO delivery systems 16

1.4 Research Objectives 18

2 Materials and Methods 19

2.1 Dual-Luciferase reporter plasmid design 19

2.2 Oligonucleotide design and synthesis 20

2.3 Agarose gel electrophoresis 20

2.4 Gibson Assembly 20
2.4.1 Plasmid linearisation 20
2.4.2 Dephosphorylation of linearised plasmid backbone 20
2.4.3 Cloning of oligonucleotides into plasmid 21
2.4.4 Bacterial transformation 21
2.4.5 Plasmid DNA extraction 21

2.5 Cell Culture 22
2.5.1 Human embryonic kidney 293T (HEK293T) cells 22

2.6 Cell transfection 22

2.7 RNA extraction 23

2.8 Plasmid linearisation 23

2.9 Polymerase Chain Reaction (PCR) 23

2.10 Reverse transcription quantitative PCR (RT-qPCR) 24
2.10.1 Synthesis of complementary DNA (cDNA) 24
2.10.2 Quantitative PCR (qPCR) 24

2.11 Dual-Luciferase assay 25

2.12 Statistical analysis 26

3 Results 27

3.1 Identifying *BDNF* transcript variants containing predicted uORFs. 27

3.2 Investigating the repressive effects of predicted uORFs on pORF expression. 29
3.3 Investigating the effects of exon deletion/s in *BDNF* transcript variants 11 and 14 on luciferase levels. 34
3.4 Investigating the mRNA levels of *BDNF* transcript variant 11 exon deletion constructs. 40
3.5 Identifying translationally repressive elements in exon 2 of *BDNF* transcript variant 11. 41
4 Discussion 51
5 References 55
6 Appendix 66

List of Tables

Table 1- Primers for quantitative PCR. 25
Table 2- Human *BDNF* sense transcript variants. 28
Table 3- 5′ UTR DNA sequences of the *BDNF* transcript variants under investigation. 34
Table 4- The length of predicted uORFs in 5′ UTRs of *BDNF* transcript variants. 35

List of Figures

Figure 1- Ribosomal processing of uORF-containing transcripts. 5
Figure 2- Exon layout of human *BDNF* sense transcript variants. 8
Figure 3- Steric-block antisense oligonucleotides mask splicing signals. 12
Figure 4- Dual-Luciferase reporter plasmid. 19
Figure 5- Dual-Luciferase reporter genes in plasmid. 29
Figure 6- The 5′ UTR of *BDNF* v5 30
Figure 7- Silencing of multiple uORFs in *BDNF* v5 causes significant increases in luciferase levels. 31
Figure 8- Silencing of multiple uORFs in *BDNF* v5 has varied effects on luciferase levels. 31
Figure 9- The 5′ UTR of *BDNF* v14 32
Figure 10- Different combinations of uORF-silencing in *BDNF* v14 have different effects on luciferase levels. 33
Figure 11-Deletion of exon 2 alone, and in combination with exon 3 in the 5′ UTR of *BDNF* v11. 36
Figure 12- Deletion of the *BDNF* v11 5′ UTR exon 2 alone and in combination with exon 3 leads to significant increases in luciferase levels. 37
Figure 13- Deletion of exon 2 in *BDNF* v14 5′ UTR. 38
Figure 14- Deletion of *BDNF* v14 5′ UTR exon 2 causes no increase in luciferase levels. .39
Figure 15- Deletion of *BDNF* v11 5′ UTR exons leads to no significant changes in mRNA levels. 40
Figure 16- Examples of tested constructs containing a uORF-silenced *BDNF* v11 5′ UTR exon 2 and deletion of HuR and Caprin1 RNA-binding motifs. 42

Figure 17- Silencing of uORFs, but not deletion of HuR or Caprin1 RNA-binding motifs in *BDNF* v11 5′ UTR exon 2, contributes to the increase in luciferase levels seen upon whole exon 2 deletion. 43
Figure 18- Sequential 50 nucleotide deletions of the 5′ UTR *BDNF* v11 exon 2 in the uORF-silenced context. 44
Figure 19- Deletion of nucleotides 1-50 and 51-100 in *BDNF* v11 5′ UTR exon 2 leads to a significant increase in luciferase levels. 45
Figure 20- Deletion of the first 50 nucleotides in exon 2 of *BDNF* v11 5′ UTR accounts for most of the increase in luciferase levels recorded upon whole exon 2 deletion.....46
Figure 21- Predicted RNA secondary structure of the 5′ UTR of *BDNF* v11 following deletion of the first 50 nucleotides in exon 2. 48
Figure 22- Sequential 10 nucleotide deletions within the first 50 nucleotides of *BDNF* v11 5′ UTR exon 2 in the uORF-silenced context. 49
Figure 23- Sequential 10 nucleotide deletions in the first 50 nucleotides of *BDNF* v11 5′ UTR exon 2 causes no significant increases in luciferase levels. 50

Abstract

Upstream open reading frames (uORFs) are found in the 5′ untranslated region (5′ UTR) of messenger RNA and are thought to repress gene expression by preventing ribosomal translation of the main coding sequence.

Brain-derived neurotrophic factor (BDNF) is a neurotrophin that plays key roles in learning and memory. Seventeen *BDNF* transcript variants are known to exist, and we predicted that 14 of these contain at least one uORF. Reduced levels of BDNF are associated with several diseases and therefore mechanisms that upregulate BDNF are needed.

We investigated the repressive potential of uORFs in *BDNF* by silencing them (adenine to thymine conversion in uORF start codons) in *BDNF* transcript variants 5 (v5) and 14 (v14). *BDNF* 5′ UTR sequences were cloned into a Dual-Luciferase reporter plasmid, human embryonic kidney 293T (HEK293T) cells were transfected, and a Dual-Luciferase assay was performed. Silencing of the second uORF in *BDNF* v14 led to significant increases in luciferase levels, whereas silencing of individual uORFs in *BDNF* v5 did not. In general, the increases in luciferase levels were greater as more uORFs were silenced.

We also deleted 5′ UTR uORF-containing exons in *BDNF* transcript variant 11 (v11) and *BDNF* v14. The deletion of exon 2 alone, and in combination with exon 3 in *BDNF* v11, led to significant increases in luciferase activity, whereas deletion of exon 2 in *BDNF* v14 did not. The silencing of uORFs and deletion of the first 50 nucleotides in *BDNF* v11 exon 2 accounted for most of the increase recorded following whole exon 2 deletion. Further work is required to identify additional translation repressive elements in the first 50 nucleotides of *BDNF* v11 exon 2. This study highlights the potential for silencing of individual uORFs and/or the skipping of uORF-containing exons as mechanisms of targeted protein upregulation.

1 Introduction

1.1 Upstream open reading frames (uORFs)

1.1.1 uORFs and the ribosome

uORFs are regulatory elements found in the 5′ untranslated region (5′ UTR) of messenger RNA (mRNA). They are believed to repress translation of the downstream protein-coding primary open reading frame (pORF). uORFs are relatively common in human transcripts and have been estimated to be present in approximately 50% of human transcripts[1,2].

Start codons, such as those in uORFs, are read by scanning ribosomes within the 43S pre-initiation complex (43S PIC), which is made up of multiple constituent parts, including the 40S ribosomal subunit, a eukaryotic translation initiation factor (eIF) 2-guanosine 5′-triphosphate (GTP)-methionine initiator transfer RNA ($tRNA_i^{Met}$) ternary complex, eIF1, eIF1A, eIF3 and eIF5[3]. The 43S PIC initiates translation by binding to the 5′-7-methylguanosine cap and scans along the mRNA transcript until it recognises a start codon (aided by eIF4A, eIF4B and eIF4F)[4]. Upon recognition of a start codon, the 43S PIC stops scanning, and forms a 48S initiation complex with strong anticodon-codon base pairing. This leads to the release of eIFs, including eIF1[5,6], causes hydrolysis of eIF2-GTP (promoted by eIF5)[7], and results in joining of the 60S subunit (promoted by eIF5B) to initiate protein translation[8].

The manner by which uORFs reduce translation of the pORF has not been fully elucidated, but it is likely that multiple mechanisms are at play. However, a general principle that underlies all the proposed mechanisms is that the presence of a uORF reduces the ability of the 43S PIC to access the start codon of the pORF (Figure 1).

Many factors are thought to affect the repressive potential of uORFs. Thus, it has been proposed that uORFs limit translation of the pORF to a greater extent when they are in a strong Kozak sequence context, when there are multiple uORFs, when uORFs are longer,

and when they are located further downstream from the 5′-7-methyguanosine cap[9]. In addition, surrounding secondary and tertiary RNA structures can also play a role in determining the repressive potential of uORFs[10].

The sequence context of uORFs is especially important, since it affects the likelihood that the 43S PIC recognises the uORF and initiates translation. As proposed by Kozak, start codons in a context most similar to GCC(**A/G**)CCAUG**G** are favourable, with the presence of purine nucleotides at positions -3 and +4 (relative to the start codon; shown in bold) being of greatest importance[11]. The Kozak context is deemed 'strong' when both -3 and +4 nucleotides are matching the consensus, it is considered to be 'intermediate' or 'adequate' as long as one of these nucleotides is present, and 'weak' when the nucleotides at these positions do not match the consensus sequence[12].

If a uORF is found within a weak sequence context, the ribosome may simply scan through the uORF, a phenomenon known as 'leaky scanning'. The recognition of the uORF is dependent on the stringency of start codon selection. The relative levels of eIF1 and eIF5 in cells can play an important role in determining this stringency. More specifically, high levels of eIF1 (relative to eIF5) promote high stringency of start codon selection and therefore increase the probability that leaky scanning of uORFs found in weak Kozak sequence contexts will occur, thus leading to increased expression of the pORF. In contrast, high levels of eIF5 (relative to eIF1) leads to a lower stringency of start codon selection and thereby promote the expression of uORFs found in weak sequence contexts[13]. In addition, low levels of eIF1 promote translation of uORFs with near-cognate start codons[14].

Ribosomal stalling during translation of a uORF is thought to repress pORF expression. Interactions between the nascent uORF-encoded peptide and ribosome can cause ribosomal stalling, resulting in a ribosomal blockade, thereby limiting translation of the pORF[15]. However, it should be noted that even following successful termination of uORF translation,

the translation of the pORF might not be efficient, since the ribosomal subunits are recycled and may not re-assemble in time to translate the pORF. Moreover, uORFs can lead to repression of the pORF by triggering the nonsense-mediated decay (NMD) pathway. This pathway serves as a safety mechanism to detect nonsense or frameshift mutations that cause premature stop codons in the 5′ UTR. The recognition of uORF stop codons by ribosomes can lead to their stalling and triggers degradation of the transcript by the NMD pathway[16]. This is supported by research showing that uORF-containing transcripts usually have shorter half-lives[2].

However, the presence of a uORF does not necessarily mean that pORF expression is repressed, because ribosomes can translate a uORF and can still re-initiate downstream translation of the pORF. This is possible when incomplete recycling of the ribosomal subunits following uORF translation occurs, such as when the larger 60S ribosomal subunit is recycled, but the 40S subunit remains bound to the mRNA[17]. The likelihood of re-initiation of translation at the pORF is greater for shorter uORFs, and when there is a greater sequence length between the uORF and the start codon of the pORF. It has been suggested that the uORF should be no more than 30 nucleotides in length (in mammals) for successful translation re-initiation at the pORF following translation of a uORF[18]. The translation of shorter uORFs increases the likelihood that the ribosome can re-initiate translation at the pORF[19].

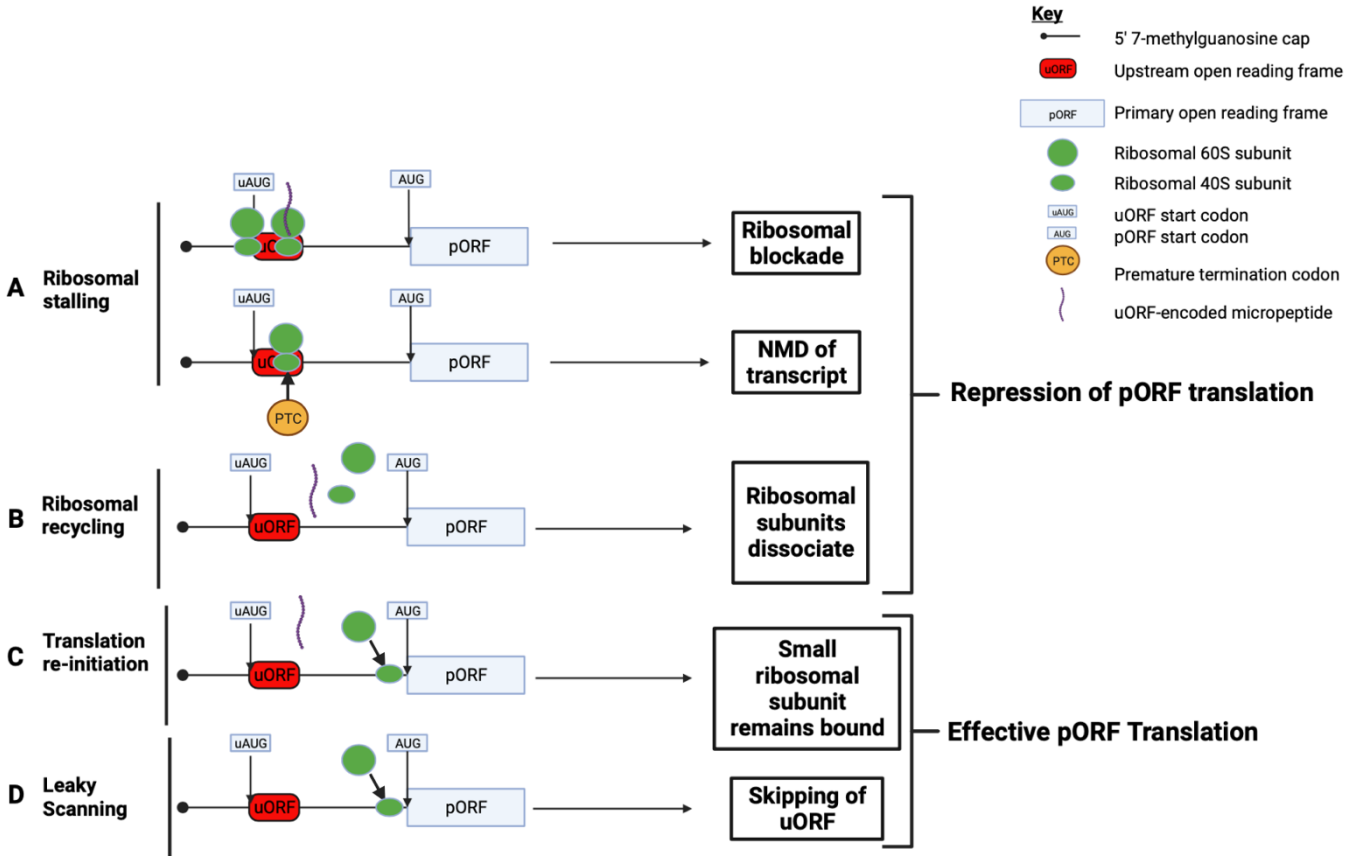


Figure 1- Ribosomal processing of uORF-containing transcripts.
(A), A uORF-encoded peptide interacts with the ribosome and leads to its stalling, causing a ribosomal blockade and reduced pORF translation. In addition, recognition of a uORF stop codon can lead to ribosomal stalling and trigger nonsense mediated decay (NMD) of the transcript. (B), Ribosomes are recycled, leading to disassociation of their subunits, which do not re-assemble in time for pORF translation. (C), The 40S ribosomal subunit remains attached to the mRNA following synthesis of the uORF-encoded peptide, allowing for re-binding of the ribosomal 60S subunit to translate the pORF. (D), uORFs found in weak Kozak sequence contexts can lead to the 40S ribosomal subunit scanning through the uORF start codon without translating it, and the 60S ribosomal subunit only binds to the 40S subunit to translate the pORF.

1.1.2 Modulatory roles of uORFs

uORF-encoded peptides can interact with proteins encoded by the same or different transcripts[20]. There are many examples of uORF-encoded peptides having functional roles, such as increasing mitochondrial fission[21], inhibiting angiotensin receptor signalling[22] and inhibiting transcription of genes involved in cell differentiation and proliferation[23]. Recently, a uORF-encoded peptide has been described that inhibits the tyrosine kinase activity of both

the protein kinase C (PKC) encoded downstream of the uORF, and of other PKC family members[24].

uORFs can also modulate the expression of pORF sequences in response to changes in the microenvironment. For example, mammalian *ATF4* promotes the translation of genes involved in amino acid biogenesis and contains 2 uORFs. The first uORF has minimal repressive effects on *ATF4* pORF translation, while the second uORF inhibits pORF expression[25]. However, upon amino acid deprivation, some of the ribosomal factors needed for translation initiation are lacking (eIF2-GTP). As a result, re-initiation of translation of the second uORF is delayed, which results in its leaky scanning, and translation only re-initiates at the pORF [26]. In addition, a uORF found in the yeast *CPA1* gene encodes an arginine attenuator peptide that senses cellular arginine levels. Binding of this uORF-encoded peptide to arginine triggers ribosomal stalling at uORF stop codons, which leads to NMD of the *CPA1* transcript [27,28].

1.1.3 uORFs in disease

Mutations that introduce a new uORF start codon, disrupt the start or stop codon of a pre-existing uORF, or alter the strength of the Kozak consensus sequence surrounding uORF start codons can lead to significant changes in protein levels[29]. For this reason, there is a strong negative selection against genetic variants that generate uORFs and those that silence uORF stop codons. This is supported by the fact that uORFs are not as common in 5′ UTRs as would be expected by chance[30]. This negative selection is most likely due to the detrimental effects that could occur as a result of uORF-induced reductions in protein levels[31].

Many disease-associated genes contain uORFs, such as the beta-site amyloid precursor protein cleaving enzyme gene (*BACE1*), which is necessary for the production of beta-amyloid and is associated with Alzheimer's disease, and the DJ-1 gene (*DJ-1*) which is

associated with Parkinson's disease[32]. A link also exists with cancer, because two-thirds of oncogenes are estimated to contain a uORF[33]. The formation of uORFs due to mutations in the 5′ UTRs of tumour-suppressor genes can lead to their reduced expression and cancer. For example, a point mutation that leads to the generation of a uORF start codon in the 5′ UTR of cyclin-dependent kinase inhibitor 2A gene (*CDKN2A*) can lead to melanoma[34]. The generation of disease-causing uORF start codons has also been reported in a cystic fibrosis transmembrane conductance regulator-related disorder[35].

Mutations that change the properties of pre-existing uORFs can also cause disease, such as the phenotype of multiple endocrine neoplasia syndrome type 4, where a deletion in a uORF present in the gene encoding cyclin-dependent kinase inhibitor 1B (*CDKN1B*) can enhance its repressive effect by increasing the uORF length due to the next in-frame stop codon now being further downstream[36]. Mutations that lead to increases in uORF sequence length reduce the likelihood of translation re-initiation at the pORF.

In contrast, the repressive effect of a uORF can also be reduced following mutations that lead to uORF shortening. For example, as reported in a case of hereditary thrombocythaemia, the generation of a stop codon further upstream as a result of a point mutation in the thrombopoietin gene (*THPO*) can lead to the shortening of a strongly repressive uORF, which increases the sequence distance to the pORF, and the likelihood that the ribosome re-initiates translation at the pORF[37,38].

1.2 Brain-derived neurotrophic factor (BDNF)

1.2.1 BDNF gene (*BDNF*)

BDNF is a member of the neurotrophin family of proteins. The human *BDNF* locus encodes 17 RefSeq-annotated transcripts (Figure 2) that are generated as a consequence of differential transcription start site usage and alternative splicing[39]. *BDNF* transcript variants consist of

different 5′ UTRs, but the same pORF. The *BDNF* pORF encodes pro-BDNF, which is the precursor of mature BDNF[40].

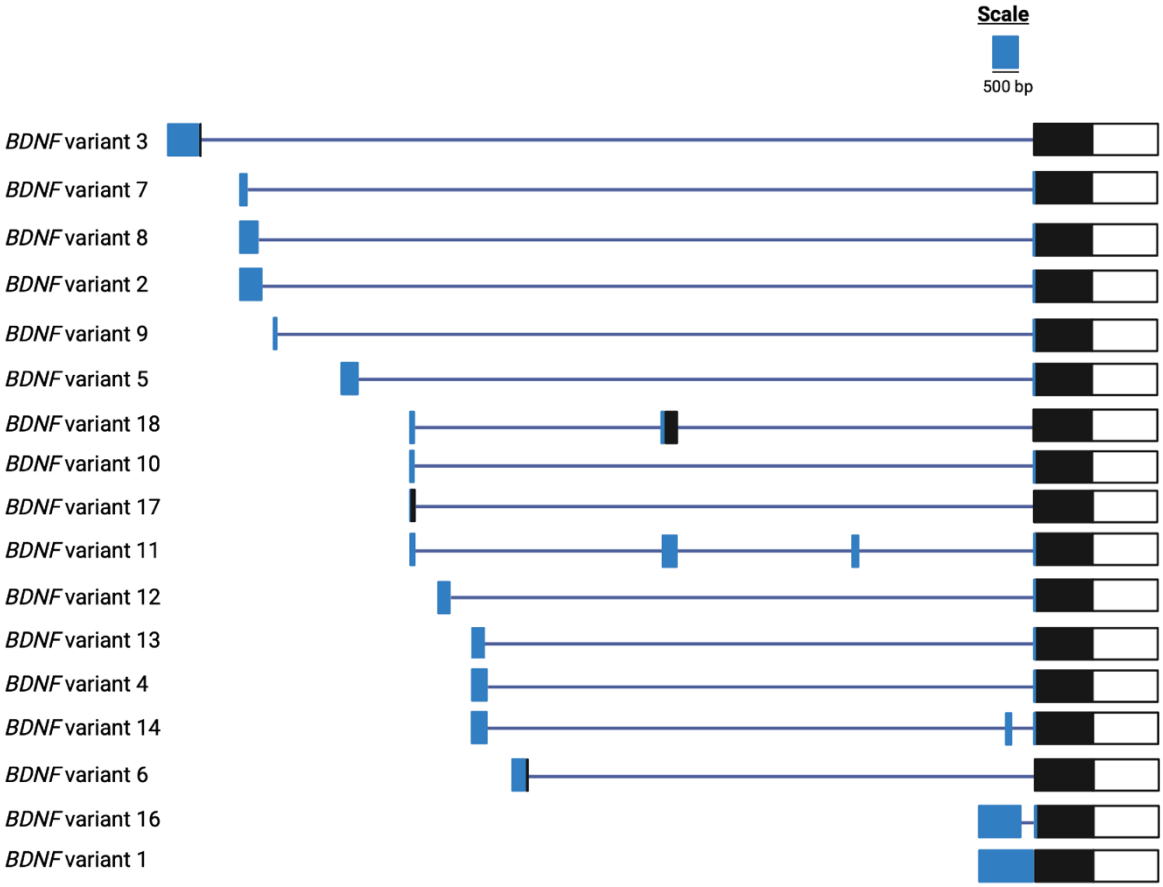


Figure 2- Exon layout of human *BDNF* sense transcript variants.
Seventeen *BDNF* sense transcript variants are known to exist. Exons shown in blue are found in the 5′ UTR, the region of exon shown in black represents the main coding sequence (pORF) and in white is the 3′ UTR. The 5′ UTR exons are drawn to scale. Adapted from Figure 1 in [39].

1.2.2 BDNF synthesis and function

Pro-BDNF is synthesised in the endoplasmic reticulum and its release can be constitutive or in response to stimuli (activity-dependent secretion)[41]. The pro-domain is proteolytically cleaved to form mature BDNF intracellularly, either by furin or proprotein convertases[42,43]. Alternatively, pro-BDNF can be converted into mature BDNF following extracellular proteolytic cleavage by metalloproteinases or plasmin[44].

Pro-BDNF has some biological activity, since it can trigger cell apoptosis by binding to p75 tumour necrosis factor (p75 TNF) receptors. However, mature BDNF is the predominant form in the nervous system[45]. It promotes neuronal cell survival and differentiation by binding to tropomyosin-related kinase B (TrK B) receptors[46,47] which are found on both pre- and post-synaptic membranes.

Mature BDNF is found in most brain regions, where it plays an important role in both the development and maintenance of the nervous system. More specifically, BDNF promotes learning and memory through increasing dendritic branching, long-term potentiation, and synaptic plasticity[48,49,50,51]. Its importance in cognitive ability has been highlighted by the fact that people with a valine/methionine polymorphism at residue 66 of BDNF have reduced secretion and suffer from poorer memory[52].

1.2.3 Current approaches for upregulating BDNF protein levels

Several neurodegenerative diseases are associated with reduced BDNF levels, including Alzheimer's disease[53,54], Parkinson's disease[55,56] and Huntington's disease[57,58]. In addition, people suffering from psychiatric disorders such as depression are thought to have reduced BDNF levels[59,60].

The upregulation of BDNF levels in models of neurodevelopmental and neurodegenerative diseases has been reported to improve some disease symptoms. For example, increasing BDNF levels in mouse models of Rett syndrome improved symptoms[61], while increasing BDNF levels reduced neuronal loss and improved disease symptoms in rodent models of Alzheimer's disease[62], Parkinson's disease[63,64] and Huntington's disease[65]. Moreover, given its neuroprotective effects, the administration of BDNF is being investigated as a possible therapeutic intervention in response to acute injuries, with the aim of limiting the extent of damage after a stroke[66] or spinal cord injuries[67].

Identifying ways to upregulate BDNF levels in brain is a challenge. Disadvantages of the peripheral administration of recombinant BDNF are its short half-life in plasma and its inability to pass through the blood-brain barrier (BBB)[68]. In fact, even if the BBB is bypassed by directly administering BDNF into the central nervous system (intrathecally or intraventricularly), it does not reach most of the brain or spinal cord, and increasing the amounts administered to improve its delivery can cause adverse effects[69]. Peptide mimetics of BDNF that bind to TrK B receptors have longer half-lives than the recombinant protein and can cross the BBB, but can still generate adverse effects as a result of causing general increases in TrK B signalling[70,71]. Moreover, the repurposing of licensed pharmacological agents such as some antidepressants[72,73] and lithium chloride[74,75] could be effective ways for increasing BDNF levels.

The delivery of constructs expressing BDNF to areas of damage could help to increase BDNF protein levels locally. In fact, delivery of *BDNF* cDNAs to specific brain regions in Alzheimer's disease (using an adeno-associated virus platform) is currently in clinical trials[76]. Moreover, antisense oligonucleotide (ASO)-mediated inhibition of natural antisense *BDNF* transcripts that repress the expression of *BDNF* sense transcript variants could upregulate BDNF levels[77]. Overall, despite advances in the ability to upregulate BDNF levels, new approaches are needed.

1.3 Antisense oligonucleotides (ASOs)

1.3.1 ASO-mediated exon skipping

ASOs are short single-stranded nucleic acid sequences that bind to complementary RNA sequences. There are two main types of ASOs that are categorised based on whether they are dependent on Ribonuclease H1 (RNase H1) action or not. ASOs that rely on the action of endogenous RNase H1 are known as gapmers and are complexes made up of an antisense DNA region with flanking modified RNA-like nucleotides on either side. Gapmers bind to a

complementary target mRNA transcript, and upon formation of a DNA-RNA heteroduplex, trigger RNase H1-mediated degradation of the transcript.

In contrast, steric block ASOs are RNase H1-independent and solely consist of RNA-like residues. The binding of steric-block ASOs to target transcript sequences does not trigger RNA degradation, but masks RNA sequences. For exon skipping, steric block ASOs mask splice sites and thereby prevent binding of the spliceosome (Figure 3). Steric block ASOs can be used for the skipping of exons that contain damaging mutations or for the skipping of exons to modify translational reading frames. A number of Food and Drug Administration (FDA)-approved ASO-mediated exon skipping treatments are in the clinic. For example, steric block ASOs designed to skip exons 45 (casimersen), 51 (eteplirsen) and 53 (golodirsen or viltolarsen) of the Dystrophin gene (*DMD*) are being used for the treatment of Duchenne muscular dystrophy (DMD).

Steric block ASOs can target two main sequence types within pre-mRNAs to modulate splicing. (i) Splice acceptor and donor consensus sequences that consist of AG and GT dinucleotides at exon-intron junctions, (ii) Cis-elements found in introns and exons called intronic/exonic splicing enhancers (ISE/ESEs) and intronic/exonic splicing silencers (ISS/ESSs)[78,79]. Serine-arginine rich (SR) proteins bind to splicing enhancer sequences and promote inclusion of the exon, while splicing silencer sequences are often bound by heterogenous nuclear ribonucleoproteins (hnRNPs) that promote exon exclusion from the mature mRNA[80]. The ability of steric block ASOs to cause exon skipping by targeting a variety of splicing signals within pre-mRNAs allows for the potential application of this technology in different contexts.

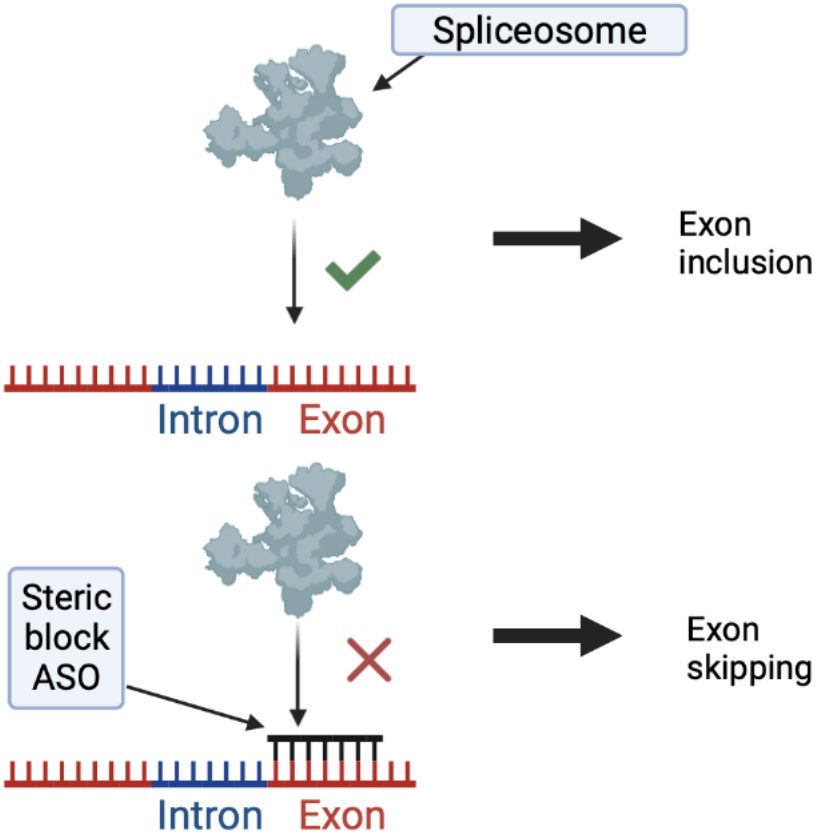


Figure 3- Steric-block antisense oligonucleotides mask splicing signals.
Masking of splice sites or intronic/exonic splice site enhancer sequences in pre-mRNA by steric-block antisense oligonucleotides (ASOs) can prevent the spliceosome from incorporating target exons, leading to exon skipping.

There are many different applications of ASO-mediated exon skipping technology that have already been investigated. For example, ASOs have been successfully used to restore the levels of β-globin in β-thalassaemia by correcting aberrant splicing of the β-Globin gene (*HBB*) following the activation of cryptic splice sites by mutations[81].

The use of steric block ASOs may also prove useful when exonic mutations cause loss of protein expression. For example, in most cases of DMD, deletions that disrupt the translational reading frame occur within two main regions of *DMD* (between exons 2-20 and exons 45-55)[82], and lead to the production of non-functional dystrophin. The use of steric block ASOs for the skipping of a *DMD* exon containing these deletions can restore the reading frame, and lead to the production of truncated, functional dystrophin. Moreover, the

administration of several ASOs to skip multiple exons at once, in a so-called 'ASO cocktail', could be used to treat DMD sufferers with a variety of disease-causing mutations[83].

Like RNase H1-dependent ASOs, steric block ASOs can also rely on cellular processes to fulfil their functions. Specifically, steric block ASOs can (indirectly) interfere with the NMD pathway to modulate expression of target mRNAs. Thus, steric block ASOs have been used to prevent NMD of a cystic fibrosis transmembrane conductance regulator transcript (*CFTR*) by skipping *CFTR* exon 23 which contains a nonsense mutation that would trigger NMD[84]. NMD can also be taken advantage of by steric block ASOs to downregulate the expression of transcripts with unfavourable effects. The generation of premature stop codons as a consequence of steric block ASO-induced aberrant splicing can serve as a way of triggering NMD of the transcript[85].

Steric block ASO-mediated pre-mRNA splicing modulation can also be used in spinal muscular atrophy (SMA), where homozygous loss of the survival of motor neuron 1 gene (*SMN1*) results in a lack of survival motor neuron (SMN) protein[86]. The main transcript of *SMN2*, a paralog of *SMN1*, lacks exon 7, because of a cytosine-to-thymine change[87,88] within an exonic splicing enhancer, leading to the production of a truncated and non-functional SMN protein[89]. However, as a result of alternative mRNA splicing, approximately 10% of *SMN2* transcripts include exon 7 and therefore encode a fully functional SMN protein. Steric block ASOs (nusinersen) are being used to alter the splicing of SMN2 and increase the production of exon 7-containing transcripts by binding to an intronic splicing silencer motif near the 5′ splice site of intron 7[90,91]. These ASOs sterically hinder hnRNPs from promoting the splicing out of exon 7, thus increasing the formation of functional SMN protein[92].

Steric block ASOs can upregulate protein levels by targeting different elements within pre-mRNAs. They can limit translation by targeting the 5′-7-methylguanosine cap, thus inhibiting the formation of translation initiation complexes[93]. Steric block ASOs can also

upregulate the levels of some proteins by re-directing polyadenylation to cryptic splice sites, which results in more stable transcripts (that contain fewer destabilisation elements), and increased protein production[94].

The targeting of uORFs with ASOs holds promise as a method for increasing protein levels. It has been reported that ASO-mediated targeting of uORF start codons can lead to substantial increases in protein levels[95]. Moreover, in theory, uORF start codons could be silenced by adenosine deaminases acting on RNA (ADAR) enzymes that substitute the adenine of a uORF start codon into an inosine (read as guanosine)[96]. In particular, the conjugation of ADAR recruiting domains to ASOs could enable silencing of target uORF start codons by ADAR enzymes.

1.3.2 Targeting of ASOs

Despite advances in ASO exon skipping therapies, there are still many challenges that limit their use for the treatment of disease. For instance, one needs to ensure that ASOs reach the target sites at high enough concentrations to facilitate their therapeutic effects. Systemically administered ASOs face many challenges, such as entering target organs and specific cell types there, as well as avoiding clearance and degradation. Chemical modifications of ASOs, including of the backbone, ribose sugar and nitrogenous base have helped to improve their delivery.

1.3.2.1 ASO backbone chemical modifications

Chemical modification of the sugar-phosphate backbone has improved the delivery of ASOs. Since the phosphodiester bonds that link sugars in the RNA backbone are easily degraded, replacement of a non-bridging oxygen atom (in a phosphate group) with a sulphur atom to form a phosphorothioate backbone (first-generation ASO) has improved the resistance of ASOs to degradation by nucleases[97]. Moreover, phosphorothioate linkage-containing ASOs have longer half-lives as a result of their increased binding to plasma proteins (more than

95% of ASOs in biological fluids are bound to plasma proteins[98]). This increased binding allows for improved delivery and exposure of the drug at the target site. Without these linkages, ASOs would be removed by glomerular filtration before they can reach their target tissues. In addition, the phosphorothioate backbone facilitates delivery of the ASO to the nucleus[99,100], which allows exon skipping ASOs to access pre-mRNAs.

The replacement of an oxygen atom with a sulphur atom to form ASOs containing phosphorothioate backbones creates a chiral centre and the formation of many stereoisomers. These stereoisomers have varying pharmacological properties, which affect their efficacies, and so the identification of the most potent stereoisomers will, in theory, allow for a more effective therapy with lower dosage requirements[101].

1.3.2.2 ASO ribose sugar chemical modifications

Ribose sugars in ASOs can be chemically modified at the carbon atom at the 2′-O position. The 2′ nucleophilic hydroxyl group of first-generation ASOs can be replaced with a variety of more stable substituents such as a methyl group to form 2′-O-Methyl (2′-OMe), a methoxy-ethyl group to form 2′-O-Methoxyethyl (2′-MOE), or a fluorine atom to form 2′-Fluoro (2′-F). These modifications can serve to counteract the non-specific binding of phosphorothioate backbones, because the 2′ modifications improve binding affinities of ASOs to the target sequences by promoting conformational changes in ribose[102]. Moreover, these 2′ modified ASOs are more resistant to degradation by nucleases (except for 2′-F modified ASOs)[103].

More recently, third-generation ASOs with modifications that cause increased conformational constraint to enable greater binding affinities to target sequences have been designed. Examples include the addition of a methylene bridge between the 2′ oxygen and 4′ carbon of the ribose ring to make locked nucleic acids (LNA) ASOs or the addition of an

ethylene bridge between carbons at positions 3′ and 5′ in the ribose ring fused to a cyclopropane ring to make tricyclo-DNA (tcDNA) ASOs[104,105].

Third-generation ASOs can also be synthesised by replacing entire structures found in previous ASOs. For instance, phosphorodiamidate morpholino oligomers (PMOs) are synthesised by replacing the ribose ring and phosphodiester linkages with a morpholino ring and uncharged phosphorodiamidate linkages. Alternatively, peptide nucleic acid (PNA) ASOs can be made by replacing the negatively charged sugar-phosphate backbone with an uncharged synthetic polyamide backbone, forming amide linkages[106]. Third-generation ASOs are particularly effective at steric-blocking of exons, and the four FDA-approved exon skipping drugs for DMD are PMOs. The advantages of these ASOs are that they are highly resistant to nuclease degradation and have reduced non-specific binding due to their neutral charge, thereby limiting their toxicity[107]. However, their lack of charge can mean that they don't bind as effectively to plasma proteins and are more easily excreted[108]. Therefore, delivery systems may play a pivotal role in enhancing the therapeutic benefit of third-generation ASOs in certain disease contexts.

1.3.3 ASO delivery systems

The delivery of ASOs to the target tissue remains a significant challenge. ASOs must not only reach the correct tissues, but also need to pass the plasma membrane, and upon internalisation, be able to escape lysosomal degradation.

Current FDA-approved ASO therapies are chemically modified 'naked' ASOs that do not rely on delivery systems to reach their targets. ASOs can be delivered to brain and spinal cord through intrathecal administration, and to the eye by intravitreal injections. Targeting of ASOs to the liver is also effective due to the wide fenestrations in the liver endothelium[109]. Nevertheless, the use of tagged chemical conjugates and/or delivery vehicles could serve to increase delivery of ASOs across the vascular endothelium, plasma membrane and

membrane barriers within cells[110]. Improved delivery is important because it could allow for the use of lower doses, which in turn would reduce toxicity.

Cell-specific targeting of ASOs can be facilitated through conjugation to receptor ligands. A particular adaptation that has significantly improved the delivery of ASOs to hepatocytes is through conjugation to acetylgalactosamine (GalNAc)[111,112]. GalNac is a ligand that binds to the asialoglycoprotein receptor (AGPR) which is highly expressed on the hepatocyte cell-surface (approximately 500,000 receptors per hepatocyte[113]).

The use of antibody conjugates could also offer cell-specific delivery of ASOs. Antibodies are beneficial for ASO-targeting due to their high specificity and long half-life[114]. In addition, oligonucleotides of varying lengths that form three-dimensional conformations which mimic antibodies (so-called aptamers) could also be used as drug conjugates. Aptamers have lower immunogenicity than antibodies and thus reduce the risk of triggering an immune response[115].

Carrier-based systems such as nanocarriers also hold particular promise. There are a variety of different nanocarrier types, such as lipid-based nano-drug delivery systems, spherical nucleic acids, exosomes, and DNA nanostructures.

Lipid-based nanoparticle delivery systems are divided into two main categories- lipoplexes and liposomes. Lipoplexes are cationic lipids that form electrostatic interactions with polyanionic nucleic acids, whereas liposomes are lipid vesicles that can encapsulate hydrophilic nucleic acids and protect them from degradation[116]. Liposomes are more stable than lipoplexes, but they often require modifications to prevent degradation by the immune system such as through conjugation to poly(ethylene glycol) (PEG)[117]. However, administration of PEG can generate anti-PEG antibodies which will limit the efficacies of PEG-containing therapies administered in future[118]. Hence, other liposomal modifications are being investigated[119].

DNA nanostructures can also be used as delivery vehicles. For example, a DNA nanostructure (DNA origami) made from synthetic DNA oligonucleotides and a polyhedral DNA nanostructure (DNA cage) can present ASOs on their surface. DNA origami offers a method in which the design can be modified in various ways to achieve specific physical properties that will optimise delivery to the target[120].

However, a major limitation of existing delivery vehicles is their inability to cross the BBB. The use of naturally occurring extracellular vesicles called exosomes might be a way to circumvent this problem[121], but further work is needed to improve exosome-mediated delivery of ASOs, including the identification of methods that increase their drug-loading capacity[122].

1.4 Research Objectives

This thesis investigates the repressive potential of uORFs in *BDNF* transcript variants, as well as examining the effects of deleting uORF-containing 5′ UTR exons on the expression of the downstream pORF. We aim to do this by:

1. Identification of *BDNF* transcript variants that contain predicted uORFs and investigation of their repressive potential.

2. Identification of *BDNF* transcript variants with the potential for skipping of 5′ UTR exons.

3. Modelling of exon skipping by deleting exons in selected *BDNF* transcript variants and assessment of the effects using Dual-Luciferase reporter constructs.

2 Materials and Methods

2.1 Dual-Luciferase reporter plasmid design

To investigate the effect of 5′ UTRs on protein expression, a Dual-Luciferase reporter plasmid (designed by Dr Thomas Roberts) was used called pDLR 5′ UTR. The presence of a *BsmBI*-restriction site allowed for the seamless insertion of the relevant *BDNF* 5′ UTR (Figure 4). The *Renilla* luciferase gene is directly downstream of the inserted 5′ UTR sequence, and both are under the control of a simian virus 40 (SV40) promoter. pDLR 5′ UTR also contains a Firefly luciferase gene, which is under the control of a herpes simplex virus thymidine kinase (HSV-TK) promoter. The *Renilla* luciferase and Firefly luciferase genes were human codon-optimised to improve the efficiency of translation in human embryonic kidney 293T (HEK293T) cells. In addition, the plasmid contains an ampicillin-resistance gene, which is key for selecting successfully transformed bacterial colonies.

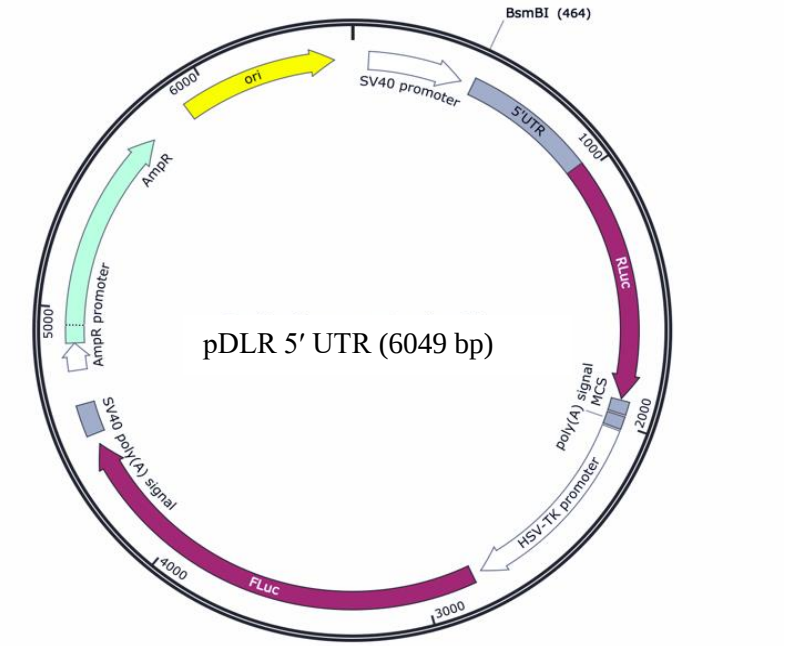


Figure 4- Dual-Luciferase reporter plasmid.
The Dual-Luciferase reporter plasmid contains a 5′ UTR insert site (pDLR 5′ UTR) and is made of 6049 nucleotides. It consists of a *Renilla* luciferase gene (*RLuc*) under the control of a simian virus 40 promoter (SV40) and its expression is modulated by an inserted 5′ UTR sequence. The 5′ UTR sequence has 5′ and 3′ overhangs to facilitate insertion into the *BsmBI* cut site in pDLR 5′ UTR by Gibson Assembly. A Firefly luciferase gene (*FLuc*) is found under the control of a herpes simplex virus thymidine kinase promoter (HSV-TK). Both the *Renilla* luciferase and Firefly luciferase genes in pDLR 5′ UTR are human codon optimised.

2.2 Oligonucleotide design and synthesis

BDNF transcript variant 5′ UTR sequences were analysed using SnapGene (Dotmatics, Boston, Massachusetts, USA) and the relevant sequences were synthesised (Integrated DNA Technologies, Coralville, Iowa, USA).

2.3 Agarose gel electrophoresis

A 2% agarose gel was made with agarose powder (Thermo Fisher Scientific, Waltham, Massachusetts, USA) and 1× TAE buffer (Thermo Fisher Scientific). Ethidium bromide (Merck, Darmstadt, Germany) was used to visualise DNA bands. DNA ladder (GeneRuler DNA Ladder Mix; Thermo Fisher Scientific) and PCR products were loaded into the wells, and gel electrophoresis was performed at 100 V for 60 min.

2.4 Gibson Assembly

2.4.1 Plasmid linearisation

BsmBI (10 U/µl; New England Biolabs, Ipswich, Massachusetts, USA) was used to linearise 1 µg of pDLR 5′ UTR backbone. This reaction was performed using 10× Tango buffer (Thermo Fisher Scientific) and made up to 20 µl with nuclease-free water. The reaction was incubated at 55°C for 1 h and then at 80°C for 20 min to heat inactivate *BsmBI*.

2.4.2 Dephosphorylation of linearised plasmid backbone

BsmBI-digested plasmid (20 µl) was dephosphorylated using antarctic phosphatase (New England Biolabs). This reaction was performed using 10× antarctic phosphatase buffer (New England Biolabs) and made up to 30 µl with nuclease-free water. It was incubated at 37°C for 30 min, and then at 80°C for 2 min to heat inactivate the enzyme. The linearisation of the dephosphorylated *BsmBI*-digested plasmid was confirmed by agarose gel electrophoresis, and the cut plasmid was purified using the GeneJet PCR Purification kit (Thermo Fisher Scientific).

2.4.3 Cloning of oligonucleotides into plasmid

For single-fragment Gibson assembly, the oligonucleotide insert was added at a 3:1 molar ratio relative to the amount of *BsmBI*-linearised plasmid. In addition, 10 µl of 2× Gibson assembly master mix (New England Biolabs) was added, and the reaction was made up to 20 µl with nuclease-free water. The mixture was then incubated at 50°C for 15 min. For two-fragment Gibson assembly, the same procedure was carried out (3:3:1 molar ratio; fragment 1: fragment 2: plasmid).

2.4.4 Bacterial transformation

DH5-alpha competent *E.coli* cells (25µl) were incubated with 1µl of the plasmid (following Gibson assembly) on ice for 30 min. Bacteria were then heat-shocked at 42°C for 45 s, and put back on ice for 2 min. The transformed bacteria were then added to 0.5 ml of SOC outgrowth medium (New England Biolabs) and incubated at 37°C for 1 h. Following this, the mixture was centrifuged at 5000 rpm for 3 min. Half of the supernatant was removed, and the pellet resuspended in the remaining liquid. The bacterial suspension was then spread on a pre-warmed ampicillin-containing (1 ng/µl) agar plate using a plate spreader. The plate was incubated overnight at 37°C. A single colony was picked and added to 5 ml Luria broth (LB) containing ampicillin (1 ng/µl), followed by growth at 37°C for 24 h.

2.4.5 Plasmid DNA extraction

Bacterial cultures were centrifuged at 5000 rpm for 3 min, and the pellets collected. Plasmid DNA was extracted using the QIAprep Spin miniprep kit protocol (Qiagen, Hilden, Germany). DNA concentrations were measured using a NanoDrop 2000 spectrophotometer (Thermo Fisher Scientific), and the plasmid DNA sequence verified by Sanger sequencing (Source BioScience, Nottingham, UK).

2.5 Cell Culture

2.5.1 Human embryonic kidney 293T (HEK293T) cells

HEK293T cells were grown in a humidified incubator at 37°C (5% CO2). They were grown in Dulbecco's Modified Eagle Medium (DMEM; Thermo Fisher Scientific) containing glucose that was supplemented with 10% Fetal Bovine Serum (FBS; Thermo Fisher Scientific) as well as 1% Penicillin, Streptomycin and Amphotericin B (PSA; Thermo Fisher Scientific). Cells were regularly checked and confirmed negative for Mycoplasma infection by PCR. For splitting and seeding of confluent cell cultures, medium was removed, cells were washed with phosphate-buffered saline (PBS; Thermo Fisher Scientific) and detached using TrypLE Express Enzyme (Thermo Fisher Scientific).

2.6 Cell transfection

In a 24-well plate (for preparation of lysates for RNA extraction), HEK293T cells were plated at 1×10^5 cells (in DMEM with 10% FBS) per well in a 24-well plate and incubated at 37°C. After 24 h, the cells were transiently transfected with 500 ng/well of the relevant pDLR 5′ UTR plasmid using polyethylenimine (PEI; Sigma-Aldrich, St. Louis, Missouri USA) transfection reagent. PEI was used at a weight:weight ratio of 4:1 relative to DNA (PEI:DNA), and left for 20 min in DMEM (no supplements) to allow for PEI-DNA complexes to form. The medium was removed 24 h later, and the cells washed with 1 ml of PBS. Then, 200 µl of TrypLE Express Enzyme was added to each well and the cells were incubated at 37°C for 2 min to allow them to detach. Following this, 2 ml of DMEM containing 10% FBS was added. The cells were then transferred to a microcentrifuge tube, and centrifuged at 1500 rpm for 5 min. The supernatant was discarded, and the pellet was kept for RNA extraction.

Cell transfection was also carried out in 96-well plates (for a Dual-Luciferase assay). HEK293T cells were plated at 2×10^4 cells per well (in DMEM with 10% FBS) and incubated

at 37°C. After 24 h, the cells were transiently transfected with 100 ng/well of the relevant pDLR 5′ UTR plasmid using PEI (weight:weight ratio of 4:1 relative to DNA).

2.7 RNA extraction

To extract RNA from transfected HEK293T cells, the Maxwell RSC simplyRNA Tissue Assay kit (Promega, Madison, Wisconsin, USA) was used. For each tested sample, an elution tube containing 50 µl of nuclease-free water and a cartridge were loaded, as set out in the manufacturer's protocol. DNase I solution (5 µl) was added to well 4 of the cartridge. Cell pellets were re-suspended in 200 µl of pre-chilled homogenisation solution which contained 1-Thioglycerol. Subsequently, 200 µl of lysis buffer was added to each sample, and the tubes were vortexed for 15 s. The lysate (400 µl) was then added to the first well of the cartridge and the simplyRNA Tissue protocol was performed to extract RNA. RNA concentrations were measured using a NanoDrop 2000 spectrophotometer (Thermo Fisher Scientific).

2.8 Plasmid linearisation

To reduce the risk of plasmid backbone concatemerisation, 1 µg of the relevant pDLR 5′ UTR was linearised with 1µl of *XbaI* (20 U/µl; New England Biolabs), 3µl of 10× rCutSmart buffer (New England Biolabs), and made up to 30 µl with nuclease-free water. This mixture was incubated at 37°C for 1 h, and then at 85°C for 15 min to heat inactivate the *XbaI*. Successful digestion was confirmed by agarose gel electrophoresis, followed by purification of the cut plasmid using the GeneJET PCR purification kit according to manufacturer's instructions.

2.9 Polymerase Chain Reaction (PCR)

PCR was also used to generate desired 5′ UTR sequences. This was achieved by adding 1µl of *XbaI*-cut plasmid (10 ng/µl), 1µl of forward primer (10 µM), 1 µl of reverse primer (10 µM), 10 µl of 2× KAPA HiFi HotStart ReadyMix (Roche, Basel, Switzerland) and brought

to 20 µl with nuclease-free water. This mixture was incubated at 95°C for 3 min for 1 cycle, and then 35 cycles at 98°C for 20 s, 55°C for 15 s and 72°C for 30 s, followed by 1 cycle at 72°C for 3 min. The PCR product was cloned directly into the pDLR 5′ UTR by single-fragment Gibson Assembly.

For two-fragment Gibson assembly, 2 PCR products with overlapping regions were generated from 2 independent PCR reactions. These overlapping regions allowed their joining upon assembly into the pDLR 5′ UTR. See Table A1 to find the primer sequences used.

2.10 Reverse transcription quantitative PCR (RT-qPCR)

2.10.1 Synthesis of complementary DNA (cDNA)

A master mix was made using the high-capacity cDNA reverse transcription kit (Thermo Fisher Scientific) which contained 10× RT buffer, 10× RT random primers, 25× dNTP mix (100 mM), MultiScribe RT (50 U/µl) and nuclease-free water. Then, 10 µl of this master mix was added to 10 µl of RNA sample (40 ng/µl) and incubated sequentially in a thermal cycler at 25°C for 10 min, 37°C for 30 min, and 85°C for 5 min.

2.10.2 Quantitative PCR (qPCR)

Primers for *Renilla* luciferase and Firefly luciferase (Table 1) were used for each cDNA sample. Each qPCR reaction consisted of 2 µl of cDNA, 10 µl of 2× SYBR Green master mix (Thermo Fisher Scientific), 1 µl of primer master mix (10 µM) and 7 µl of nuclease-free water. Two technical replicates were carried out for each sample. A no template control was also included for each primer set, where nuclease-free water was added instead of cDNA. Quantitative PCR was performed using a StepOnePlus Real-Time PCR machine (Life Technologies, Carlsbad, USA). The cycling protocol consisted of 10 min at 95°C, and then 40 cycles of 95°C for 15 s and 1 min at 60°C. Following this, melt curve analysis was performed to confirm amplification of a single reaction product. The Pfaffl method was used

to determine relative transcript levels[123]. Pfaffl analysis was carried out under the assumption that the efficiencies of both primers used to detect *Renilla* luciferase and Firefly luciferase mRNA levels were 100% (i.e., E= 2). Finally, the *Renilla* luciferase mRNA levels were normalised to the corresponding Firefly luciferase mRNA levels and scaled to the control (such that the mean value of the control was 1).

Table 1- Primers for quantitative PCR.

Target	Forward primer (5′-3′)	Reverse primer (5′-3′)
Firefly luciferase	ACTCTAAGACCGACTACCAGG	GTAGACCCAGAGCTGTTCATG
Renilla luciferase	GTAACGCTGCCTCCAGCTAC	CCAAGCGGTGAGGTACTTGT

2.11 Dual-Luciferase assay

A Dual-Glo Luciferase assay (Promega) was performed 24 h after cell transfection in a 96-well plate. Before the assay, cells and assay reagents were equilibrated to room temperature. Firstly, approximately half of the well volume (60 µl) was removed, and the cells were mixed with Dual-Glo reagent (50 µl). The cell lysate (80 µl) for each well was transferred to a Greiner 96-well plate (Merck) and the Firefly luciferase activity recorded on a CLARIOstar luminometer (BMG Labtech, Aylesbury, UK), using the settings of no filter, no gain adjustment, and a focal height of 9 mm. The Dual-Glo reagent was then quenched through addition of 40 µl of Stop and Glo reagent (Stop and Glo reagent consists of a 1:100 dilution of Stop and Glo substrate in Stop and Glo buffer). Plates were shaken and incubated for 10 min to quench the Firefly luciferase activity and start the *Renilla* luciferase reaction. *Renilla* luciferase activity was then recorded on the CLARIOstar luminometer. The *Renilla* luciferase activity was normalised to the Firefly luciferase activity recorded for each plasmid construct. The normalised *Renilla* luciferase activity levels for each construct being investigated was then scaled to the normalised levels recorded for the control, such that the

value of the mean of the control group was returned to a value of 1. The normalised *Renilla* luciferase activity levels correlate with *Renilla* luciferase expression levels.

2.12 Statistical analysis

Statistical analysis was performed to compare normalised luciferase activity of the tested constructs to that of the given control. GraphPad Prism Software Version 9.1.0 (GraphPad Software Inc., San Diego, California, USA) was used to carry out a Student's *t*-test when comparing the luciferase levels upon deletion of exon 2 in *BDNF* transcript variant 14 (v14). In addition, an ordinary one-way analysis of variance (ANOVA), followed by a multiple comparisons test with Bonferroni correction were used to compare how luciferase levels changed upon uORF silencing and exon deletion/s. An ordinary one-way ANOVA and multiple comparisons test with Bonferroni correction were also used to compare luciferase mRNA levels upon exon deletion/s. All experiments shown are representative, with each construct having at least four replicates per experiment. Each experiment was repeated at least twice. All diagrams were created using BioRender.com and graphical representations made using GraphPad Prism Software Version 9.1.0.

3 Results

3.1 Identifying *BDNF* transcript variants containing predicted uORFs.

Seventeen RefSeq *BDNF* sense transcript variants were identified using the UCSC genome browser[124,125]. The 5′ UTR sequences of these transcripts were inspected and predicted uORFs were identified. Presence of an ATG codon in the 5′ UTR and an in-frame stop codon was required for a sequence to be defined as a predicted uORF. In total, 14 *BDNF* transcript variants were predicted to contain at least 1 uORF (Table 2).

Table 2- Human *BDNF* sense transcript variants.

BDNF Sense Transcript Variant	Isoform (RefSeq)	5′ UTR sequence length (bp)	Coding Sequence length (bp)	Number of exons in 5′ UTR	Number of uORFs in 5′ UTR	uORF exon layout (Number of uORFs in exon 1, exon2 etc)	Potential for exon skipping?
17	NM_001143809	17	831	1	0	-	✗
7	NM_001143805	157	744	2	0	-	✗
8	NM_001143806	372	744	2	0	-	✗
9	NM_001143807	77	744	2	1	(1,0)	✗
12	NM_001143812	246	744	2	1	(1,0)	✗
2	NM_170732	455	744	2	1	(1,0)	✗
10	NM_001143808	94	744	2	1	(1,0)	✗
18	NM_001143810	141	990	2	2	(1,1)	✗
6	NM_170734	262	789	1	2	(2)	✗
13	NM_001143813	295	744	2	2	(2,0)	✗
4	NM_001709	313	744	2	2	(2,0)	✗
14	NM_001143814	420	744	3	3	(2,1,0)	✓
3	NM_170731	616	768	1	3	(3)	✗
5	NM_170733	346	744	2	5	(5,0)	✗
11	NM_001143811	504	744	4	11	(1,8,2,0)	✓
16	NM_001143816	860	744	2	17	(17,0)	✗
1	NM_170735	1094	744	1	22	(22)	✗

3.2 Investigating the repressive effects of predicted uORFs on pORF expression.

Oligonucleotides containing the sequences of the relevant *BDNF* transcript variant 5′ UTRs were synthesised and cloned into *BsmBI*-cut pDLR 5′ UTR plasmids by Gibson assembly. The inserted 5′ UTR sequence modulates expression of *Renilla* luciferase (Figure 5). Firefly luciferase activity served as an internal control of transient transfection of HEK293T cells, which allowed for the normalisation of *Renilla* luciferase activity to Firefly luciferase activity.

pDLR 5′ UTR plasmids containing the relevant *BDNF* 5′ UTR were transfected into HEK293T cells and Dual-Luciferase assays were performed, which enabled quantification of both *Renilla* luciferase and Firefly luciferase activities from a given lysate.

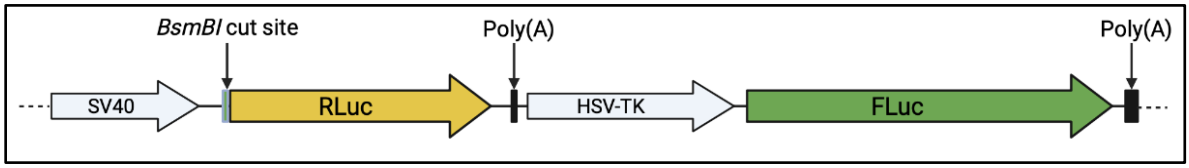


Figure 5- Dual-Luciferase reporter genes in plasmid.
A representation of a region of the Dual-Luciferase reporter plasmid (pDLR 5′ UTR) displaying the *BsmBI* cut site where the relevant *BDNF* transcript variant 5′ UTR is inserted. The 5′ UTR modulates the expression of the Renilla luciferase gene (*RLuc*) which is under the control of the simian virus 40 promoter (SV40). The Firefly luciferase gene (*FLuc*) expression is under the control of the herpes simplex virus thymidine kinase promoter (HSV-TK). The activity levels of Firefly luciferase served as an internal control.

We predicted that the 5′ UTR of *BDNF* transcript variant 5 (v5) contains 5 uORFs in exon 1 (Figure 6). To investigate their repressive effects, *BDNF* v5 5′ UTR sequences containing various combinations of silenced uORFs were cloned into pDLR 5′ UTR. Silencing of a uORF was achieved by converting the adenine of its start codon to a thymine (ATG to TTG). The normalised *Renilla* luciferase levels of the respective constructs were scaled to the normalised *Renilla* luciferase levels recorded for the plasmid containing the wild-type 5′ UTR of *BDNF* v5.

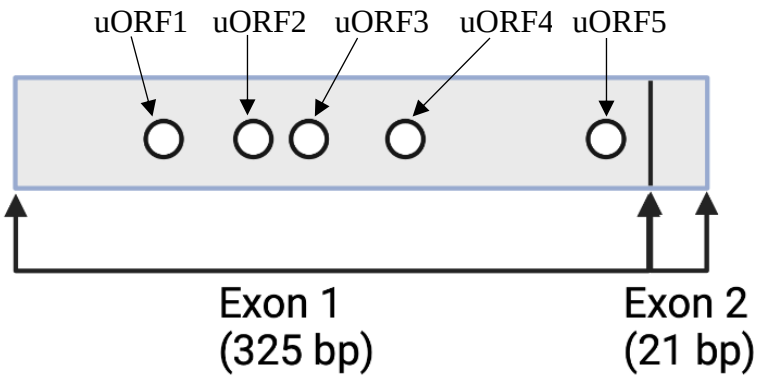


Figure 6- The 5′ UTR of *BDNF* v5.
BDNF transcript variant 5 (v5) contains 2 exons in its 5′ UTR and 5 uORFs (shown as white circles).

The silencing of individual predicted uORFs in *BDNF* v5 did not lead to significant increases in luciferase activity compared to wild-type (Figure 7). However, silencing of 2 or more uORFs led to significant increases in activity, except when uORFs 4 and 5, and/or uORFs 3,4, and 5 were silenced together (Figures 7 and 8).

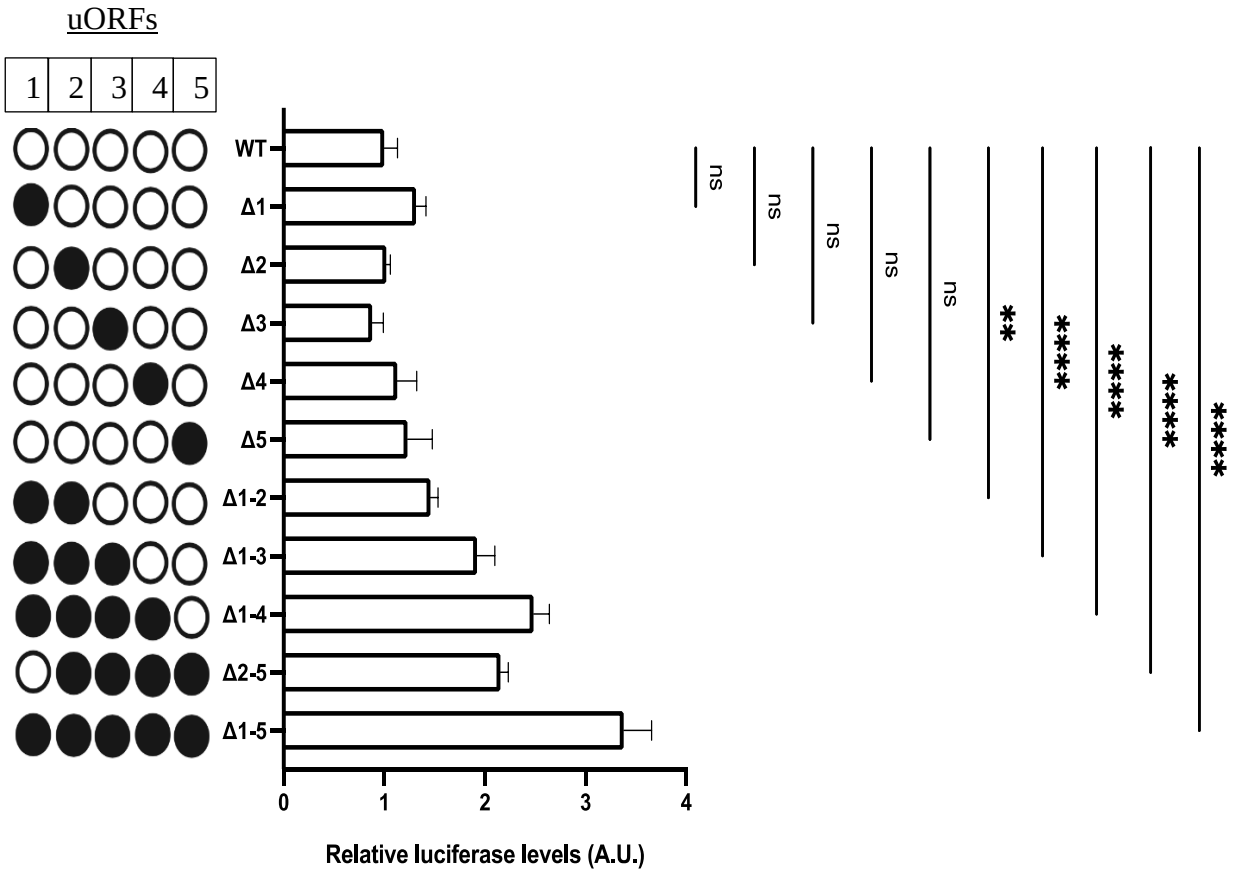


Figure 7- Silencing of multiple uORFs in *BDNF* v5 causes significant increases in luciferase levels.

Bar chart showing the effects on relative luciferase levels when silencing (ATG to TTG) predicted uORF start codons in *BDNF* transcript variant 5 (v5). *BDNF* v5 contains 5 uORFs and these are shown as white circles, while silenced uORFs are shown as black circles. The relevant *BDNF* v5 5′ UTR was inserted into a Dual-Luciferase reporter plasmid, HEK293T cells were transfected with constructs as indicated, and Dual-Luciferase reporter measurements carried out 24 h later. The recorded *Renilla* luciferase levels for each tested construct were normalised to the corresponding Firefly luciferase levels. The normalised *Renilla* luciferase levels of all tested constructs were scaled to the normalised *Renilla* luciferase levels of the *BDNF* v5 wild-type (WT) control. Statistical significance was tested by an ordinary one-way analysis of variance and *post hoc* multiple comparisons tests with Bonferroni correction. Values shown are mean + SD, with 4 replicates per construct tested. ***P* < 0.01, *****P* < 0.0001, ns = not significant.

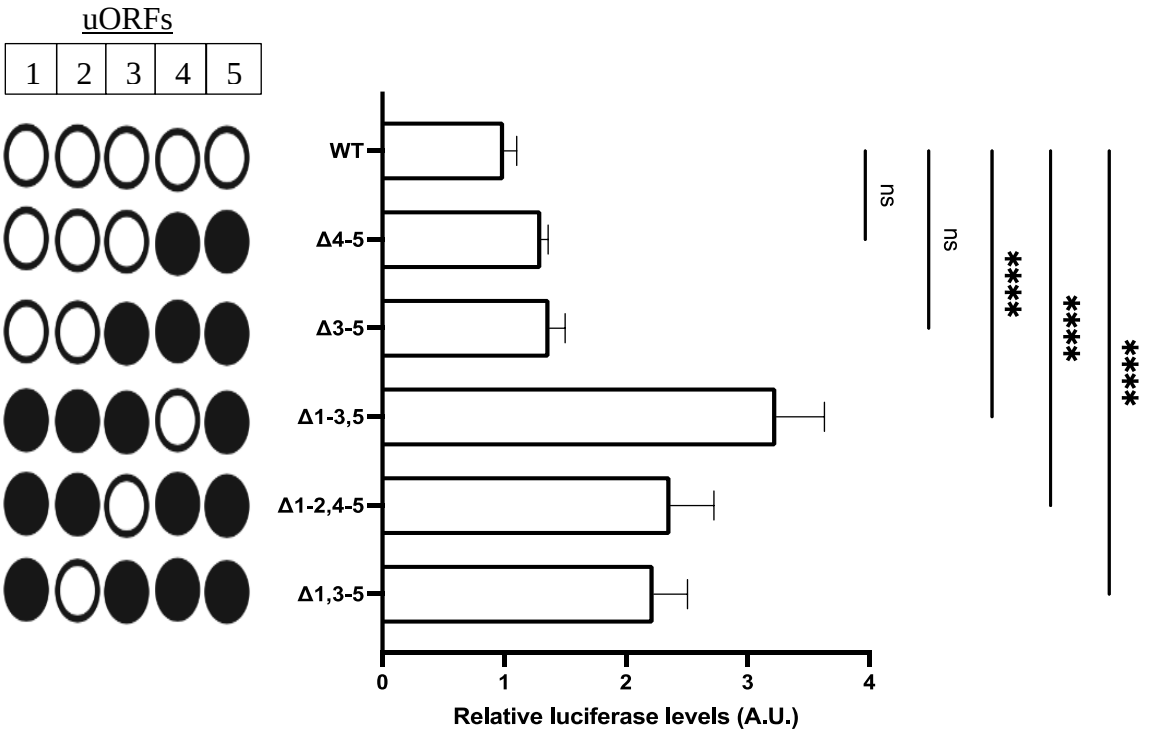


Figure 8- Silencing of multiple uORFs in *BDNF* v5 has varied effects on luciferase levels.

Bar chart showing the effects on relative luciferase levels when silencing (ATG to TTG) predicted uORF start codons in *BDNF* transcript variant 5 (v5). *BDNF* v5 contains 5 uORFs and these are shown as white circles, while silenced uORFs are shown as black circles. The relevant *BDNF* v5 5′ UTR was inserted into a Dual-Luciferase reporter plasmid, HEK293T cells were transfected with constructs as indicated, and Dual-Luciferase reporter measurements performed 24 h later. The recorded *Renilla* luciferase levels for each tested construct were normalised to the corresponding Firefly luciferase levels. The normalised *Renilla* luciferase levels of all tested constructs were scaled to the normalised *Renilla* luciferase levels of the *BDNF* v5 wild-type (WT) control. Statistical significance was tested by an ordinary one-way analysis of variance and *post hoc* multiple comparisons tests with Bonferroni correction. Values shown are means + SD, with 4 replicates per construct tested. *****P* < 0.0001, ns = not significant.

BDNF v14 contains 3 exons in its 5′ UTR, with 2 predicted uORFs in exon 1 and 1 in exon 2 (Figure 9).

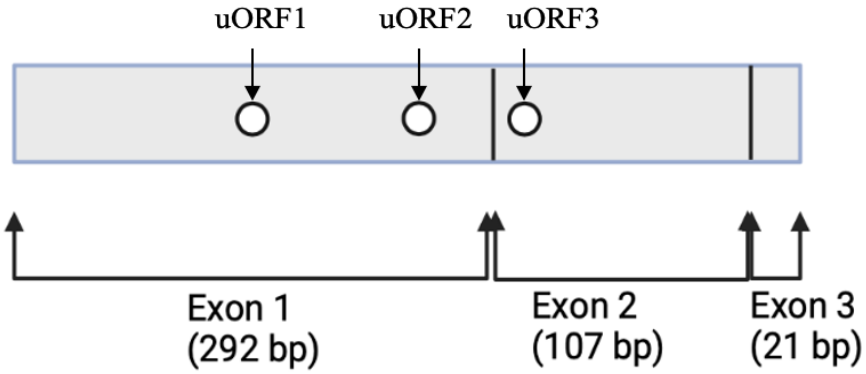


Figure 9- The 5′ UTR of *BDNF* v14.
BDNF transcript variant 14 (v14) contains 3 exons in its 5′ UTR and 3 uORFs (shown as white circles).

BDNF v14 5′ UTR sequences consisting of either individually or multiple silenced uORFs were cloned into pDLR 5′ UTR plasmids. The resulting normalised *Renilla* luciferase levels were scaled to the normalised levels for the plasmid construct containing the *BDNF* v14 wild-type 5′ UTR. Only the individual silencing of the second uORF in *BDNF* v14 led to a significant increase in *Renilla* luciferase levels compared to wild-type. In addition, significant increases in *Renilla* luciferase levels were recorded upon silencing of 2 uORFs, provided this included silencing of the second uORF. The greatest increase in luciferase levels was observed upon silencing of all 3 uORFs, although silencing of the first 2 uORFs also led to large increases (Figure 10).

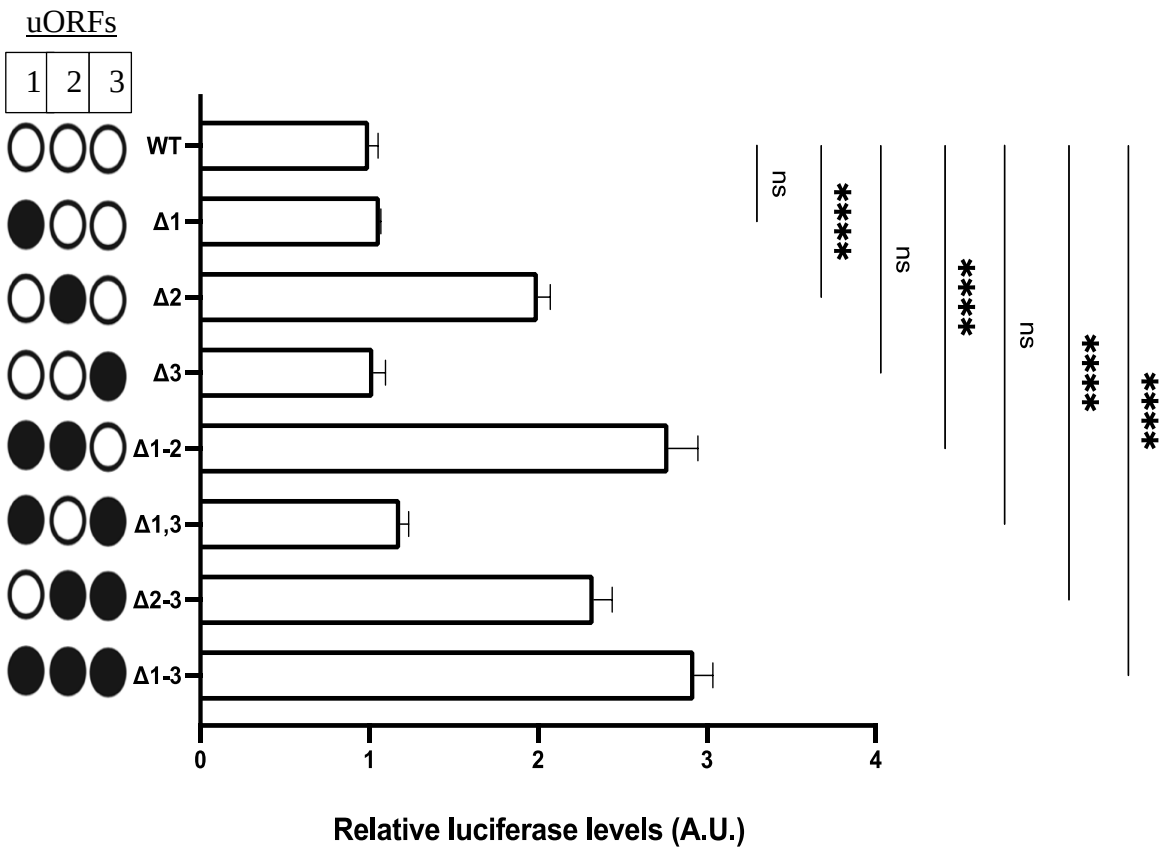


Figure 10- Different combinations of uORF-silencing in *BDNF* v14 have different effects on luciferase levels.

Bar chart showing the effects on relative luciferase levels when silencing (ATG to TTG) uORF start codons in *BDNF* transcript variant 14 (v14). *BDNF* v14 contains 3 uORFs and these are shown as white circles, while silenced uORFs are shown as black circles. The relevant *BDNF* v14 5′ UTR was inserted into a Dual-Luciferase reporter plasmid, HEK293T cells were transfected with constructs as indicated, and Dual-Luciferase reporter measurements performed 24 h later. The recorded *Renilla* luciferase levels for each tested construct were normalised to the corresponding Firefly luciferase levels. The normalised *Renilla* luciferase activities of all tested constructs were scaled to the normalised *Renilla* luciferase levels of the *BDNF* v14 wild-type (WT) control. Statistical significance was tested by an ordinary one-way analysis of variance and *post hoc* multiple comparisons tests with Bonferroni correction. Values shown are means + SD, with 4 replicates per construct tested. ****$P < 0.0001$, ns = not significant.

3.3 Investigating the effects of exon deletion/s in *BDNF* transcript variants 11 and 14 on luciferase levels.

We hypothesised that the skipping of uORF-containing exons in the 5′ UTR could upregulate BDNF levels. The criteria used to determine which *BDNF* transcripts had the potential for exon skipping were (i) the presence of at least 3 exons in the 5′ UTR, and (ii) the presence of at least 1 predicted uORF in the exon to be skipped. The first and last exons in the 5′ UTR were not considered as viable skipping targets, given that skipping them might affect the ribosome's ability to recognise, scan and translate the pORF. Two uORF-containing *BDNF* transcript variants were identified as having the potential for exon skipping, namely *BDNF* transcript variant 11 (v11) and *BDNF* v14 (Tables 3 and 4). We modelled the effect of exon skipping on protein levels, by analysing changes in luciferase levels upon exon deletion.

Table 3- 5′ UTR DNA sequences of the *BDNF* transcript variants under investigation.

***BDNF* transcript variant**	**5′ UTR DNA sequence (5′-3′)**
5	attcaccgcggagagggctgctctcgctgccgctccccccggcgaactagcatgaaatctcc ctgcctctgccgagatcaaatggagcttctcgctgatgggtgcgagtattacctccgccat gcaatttccactatcaataatttaacttctttgctgcagaacagaaggagtacataccgggc accaaagactcgcgcccctcccccctttaattaagcgaagggaacgtgaaaaaataataga gtgtgggagttttggggccgaagtctttcccggagcagctgccttgatggttactttgacaa gtagtgactgaaaag|ttccaccaggtgagaagagtg
11	gtaaaccaatagccccatgctctgtgcgatttcattgtgtgctcgcgttcgcaagctccgt agtgcaggaaggtgcgggaag|ttaagtaattaaaagaaattatagagtgggatgcaaaaat aacccgaaggacaactggatgtgtggagccaccagttttctccatgagtgcacaaggttaat ccttgttactactcagaatgctgagtttctacagaaagggttgcaggtccacacatgttttg gcgtctacccacacgcttctgtatggcatgactgtgcatcccagaagaagggctgtgctgtg tacctccacgtttcagtggaatttaacaaactgatccctgaaaatggtttcataaag|ggat ggtaataaagtctcttagtggttgaaaatgttatttcttacaaaagtggagaacatttgctt ttcaataccagagttttcagccatttctgcattctgacctattgactggag|ttccaccagg tgagaagagtg
14	gcagcctggagctccgggtccccgacgctgccgccgccgcgcccgggcgcacccgcccgctc gctgtcccgcgcaccccgtagcgcctcgggctcccgggccggacagaggagccagcccggtg cgcccctccacctcctgctcgggggctttaatgagacacccaccgctgctgtggggccggc ggggagcagcaccgcgacggggaccggggctgggcgctggagccagaatcggaaccacgatg tgactccgccgccggggacccgtgaggtttgtgtggaccccgag|catgagcagagatcatt aaaaattaaacttacaaagctgctaaagtgggaagaaggagaacttgaagccacaatttttg cacttgcttagaagccatctaatctcag|ttccaccaggtgagaagagtg

***Note- ATG nucleotides highlighted in red represent predicted uORF start codons, and the red vertical bars represent exon junctions.**

Table 4- The length of predicted uORFs in 5′ UTRs of *BDNF* transcript variants.

BDNF transcript variant	uORF number	Predicted length of uORF (bp)
v5	1	93
v5	2	63
v5	3	120
v5	4	27
v5	5	27
v11	1	78
v11	2	12
v11	3	234
v11	4	18
v11	5	141
v11	6	39
v11	7	9
v11	8	69
v11	9	12
v11	10	27
v11	11	72
v14	1	96
v14	2	6
v14	3	18

BDNF v11 has 4 exons in its 5′ UTR and we predicted there to be 1 uORF in exon 1, 8 in exon 2 and 2 in exon 3 (Figure 11). To model the skipping of exons 2 and 3 individually, and in combination, we deleted them from the *BDNF* v11 5′ UTR sequence and investigated the effects of this on luciferase activity.

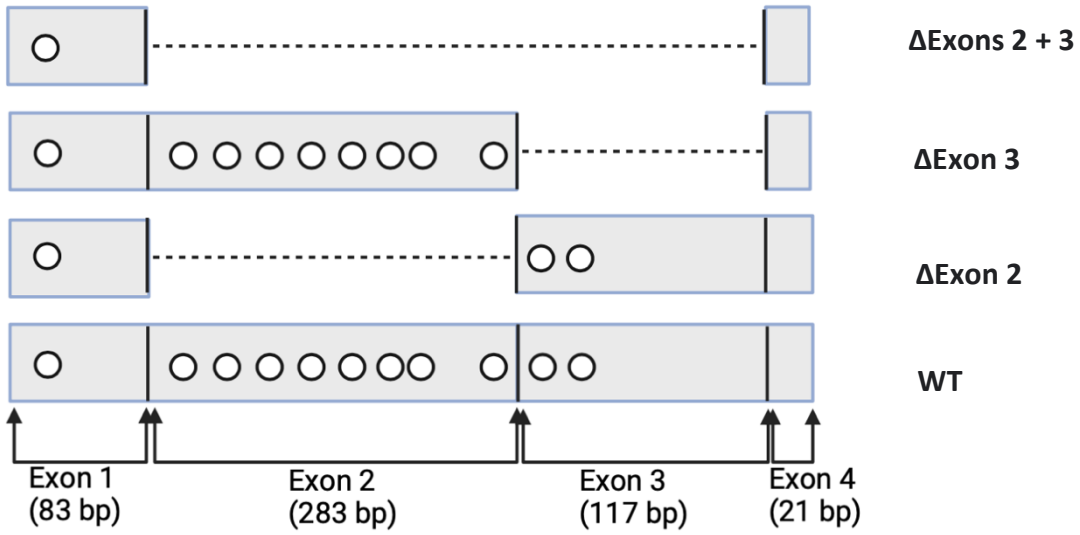


Figure 11-Deletion of exon 2 alone, and in combination with exon 3 in the 5′ UTR of *BDNF* v11.
BDNF transcript variant 11 (v11) contains 4 exons in its 5′ UTR and 11 uORFs (shown as white circles). Deleted exons are shown as dashed lines.

The normalised *Renilla* luciferase levels for these *BDNF* v11 exon deletion constructs were scaled to the levels recorded for the plasmid construct containing *BDNF* v11 wild-type 5′ UTR. Deletion of exon 2 led to a significant increase in luciferase levels, but no significant increase was recorded upon exon 3 deletion. The deletion of exons 2 and 3 led to an approximately 10-fold increase in luciferase levels compared to when exon 2 alone was deleted (Figure 12).

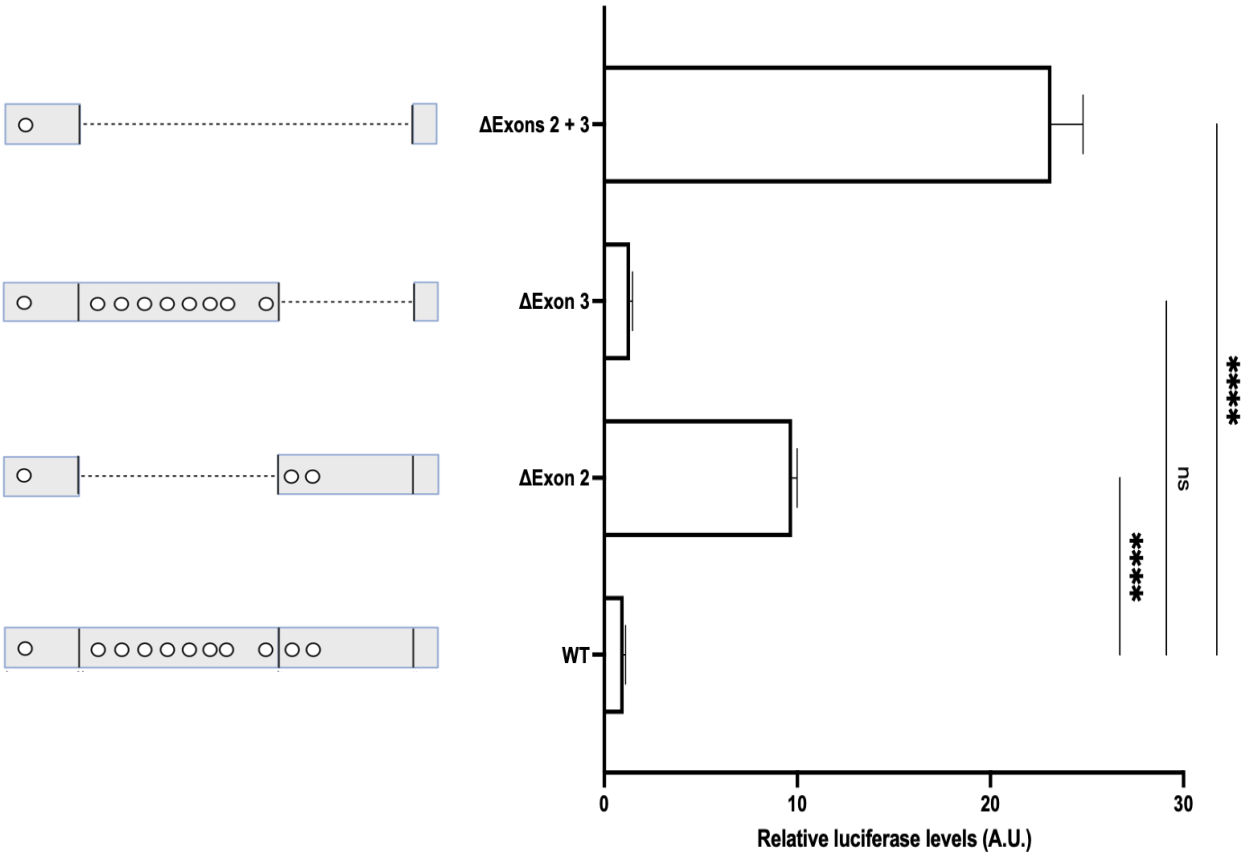


Figure 12- Deletion of the *BDNF* v11 5′ UTR exon 2 alone and in combination with exon 3 leads to significant increases in luciferase levels.

Bar chart showing the effects on relative luciferase levels when deleting *BDNF* transcript variant 11 (v11) 5′ UTR exons 2 (ΔExon 2) and 3 (ΔExon 3) individually, and in combination (ΔExons 2 + 3). The layout of *BDNF* v11 5′ UTR exons in the tested constructs is shown, with uORFs represented as white circles and deleted exons as dashed lines. The relevant *BDNF* v11 5′ UTR was inserted into a Dual-Luciferase reporter plasmid, HEK293T cells were transfected with constructs as indicated, and Dual-Luciferase reporter measurements performed 24 h later. The recorded *Renilla* luciferase levels for each tested construct were normalised to the corresponding Firefly luciferase levels. The normalised *Renilla* luciferase levels of all tested constructs were scaled to the normalised *Renilla* luciferase levels of *BDNF* v11 wild-type (WT) control. Statistical significance was tested by an ordinary one-way analysis of variance and *post hoc* multiple comparisons tests with Bonferroni correction. Values shown are means + SD, with 4 replicates per construct tested. ****$P < 0.0001$, ns = not significant.

Since *BDNF* v14 contains 3 exons in its 5′ UTR, we reasoned that the second exon could be targeted for exon skipping (Figure 13).

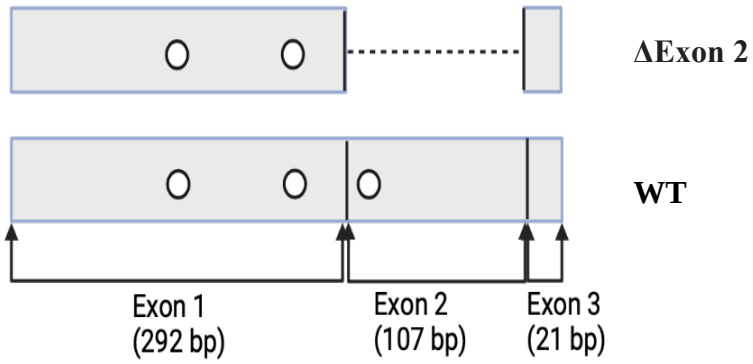


Figure 13- Deletion of exon 2 in *BDNF* v14 5′ UTR.
BDNF transcript variant 14 (v14) contains 3 exons in its 5′ UTR and 3 uORFs (shown as white circles). The deletion of exon 2 is shown as a dashed line.

The 5′ UTR sequence of *BDNF* v14 with exon 2 deleted was inserted into the *BsmBI*-cut pDLR 5′ UTR to investigate what the effects on luciferase levels would be. The effect of this exon deletion was investigated by scaling the normalised *Renilla* luciferase levels recorded for the 5′ UTR of *BDNF* v14 lacking exon 2 to the levels recorded for the plasmid construct containing the *BDNF* v14 wild-type 5′ UTR. However, deletion of exon 2 in *BDNF* v14 led to a significant decrease in luciferase levels, and therefore is probably not a good target for exon skipping-mediated BDNF upregulation (Figure 14).

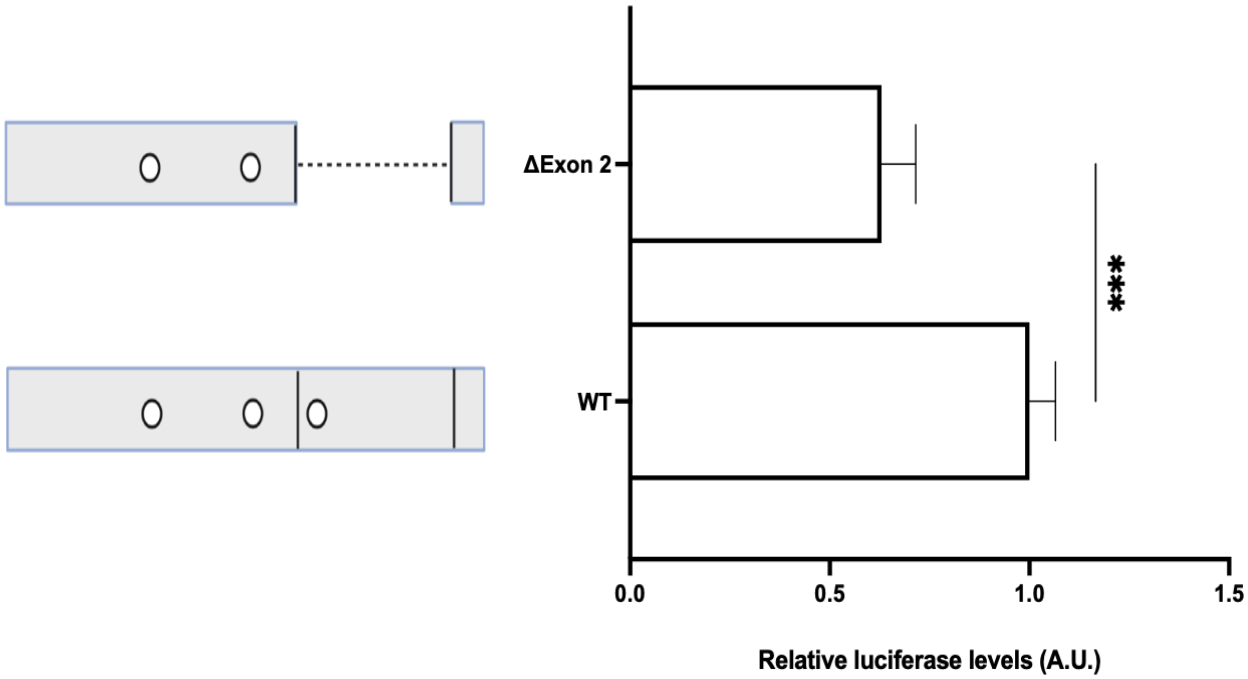


Figure 14- Deletion of *BDNF* v14 5′ UTR exon 2 causes no increase in luciferase levels.

Bar chart showing the effects on relative luciferase levels when deleting exon 2 (ΔExon 2) in the 5′ UTR of *BDNF* transcript variant 14 (v14). The layout of *BDNF* v14 5′ UTR exons in both tested constructs is shown, with uORFs represented as white circles and deleted exons as dashed lines. The relevant *BDNF* v14 5′ UTR was inserted into a Dual-Luciferase reporter plasmid, HEK293T cells were transfected with constructs as indicated, and a Dual-Luciferase reporter measurement performed 24 h later. The recorded *Renilla* luciferase levels for each tested construct were normalised to the corresponding Firefly luciferase levels. The normalised *Renilla* luciferase levels of *BDNF* v14 ΔExon 2 were scaled to the normalised *Renilla* luciferase levels of *BDNF* v14 wild-type (WT) control. Statistical significance was tested by unpaired Student's *t*-test. Values shown are means + SD, with 4 replicates per construct tested. ****P* < 0.001.

3.4 Investigating the mRNA levels of *BDNF* transcript variant 11 exon deletion constructs.

Following the transfection of HEK293T cells with plasmid constructs containing the relevant *BDNF* v11 5′ UTR, the effects on *Renilla* luciferase and Firefly luciferase mRNA levels were determined by RT-qPCR. Normalised *Renilla* luciferase mRNA levels recorded for the different exon deletion constructs were scaled to the normalised mRNA levels recorded for *BDNF* v11 wild-type. Deletion of the respective exons in *BDNF* v11 did not lead to any significant changes in mRNA levels (Figure 15).

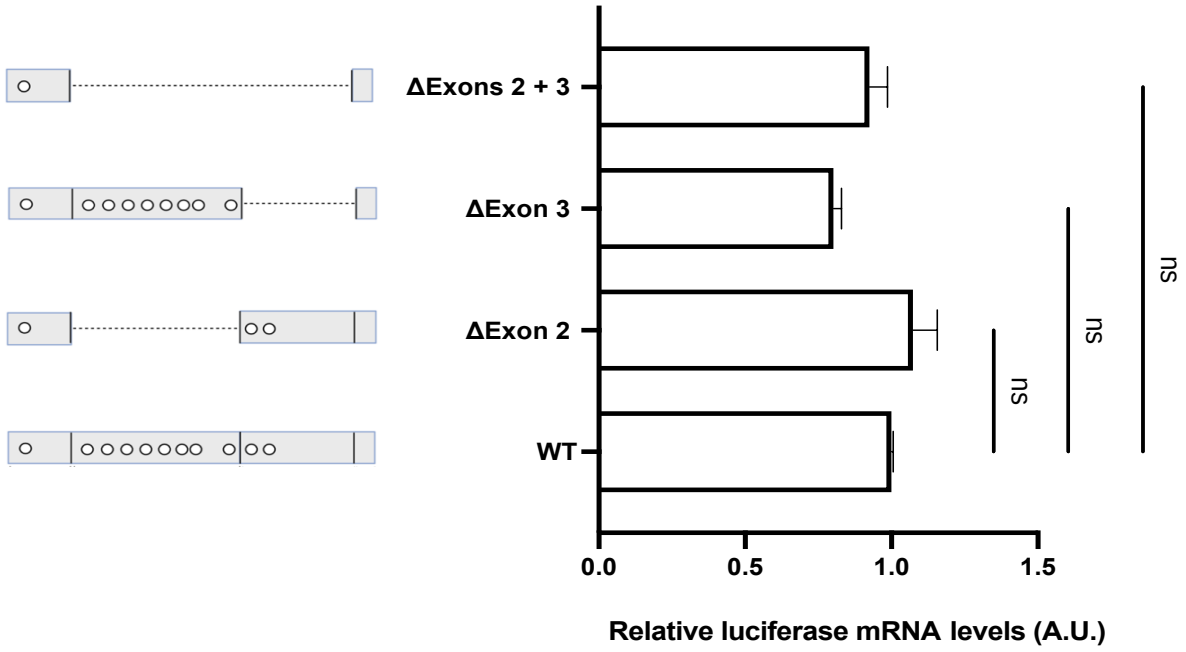


Figure 15- Deletion of *BDNF* v11 5′ UTR exons leads to no significant changes in mRNA levels.

Bar chart showing the effects on relative luciferase messenger RNA (mRNA) levels when deleting *BDNF* transcript variant 11 *(*v11) 5′ UTR exons 2 (ΔExon 2) and 3 (ΔExon 3) individually, and in combination (ΔExons 2 + 3). The layout of *BDNF* v11 5′ UTR exons in the tested constructs is shown, with uORFs represented as white circles and deleted exons as dashed lines. HEK293T cells were transfected with constructs as indicated, RNA was extracted from these cells, and mRNA levels of *Renilla* luciferase and Firefly luciferase were determined by reverse transcription quantitative PCR (RT-qPCR). The *Renilla* luciferase and Firefly luciferase mRNA levels underwent Pfaffl analysis, then *Renilla* luciferase mRNA levels were normalised to Firefly luciferase mRNA levels, and the normalised mRNA levels of all tested constructs were scaled to the normalised luciferase mRNA levels recorded for the 5′ UTR of *BDNF* v11 wild-type (WT) control. For each tested construct there were two technical replicates, and data from these technical replicates was averaged (plotted on bar chart), this was done 3 times for each construct. Statistical significance was tested by an ordinary one-way analysis of variance and *post hoc* multiple comparisons tests with Bonferroni correction. Values shown are means + SEM. Ns = not significant.

3.5 Identifying translationally repressive elements in exon 2 of *BDNF* transcript variant 11.

To determine if the 8 uORFs in exon 2 of *BDNF* v11 exert a repressive effect on the translation of the pORF, we generated a *BDNF* v11 5′ UTR sequence where these uORFs were silenced (ATG to TTG). uORF-silencing led to a significant increase in luciferase levels compared to wild-type, but this was not equal to the magnitude of increase seen upon deletion of the whole of exon 2. Therefore, in addition to uORFs, there are probably other translation repressive elements in exon 2.

We also investigated if *BDNF* v11 exon 2 may contain any RNA-binding protein motifs that could be repressing the expression of the main pORF. The use of an RNA-binding protein motif search tool called BEAM RNA Interaction mOtifs (BRIO)[126] predicted the presence of overlapping RNA-binding motifs for Human antigen R (HuR) and Cell cycle associated protein 1 (Caprin1), and an additional HuR RNA-binding motif further downstream in exon 2 (Figure 16). From here on in, I refer to the overlapping HuR and Caprin1 RNA-binding motifs as HuR-A, and the second HuR RNA-binding motif as HuR-B.

pDLR 5′ UTR constructs were generated that contained the *BDNF* v11 5′ UTR with the predicted HuR-A and Caprin1 overlapping motifs or HuR-B motif deleted individually, and in combination, in both wild-type and uORF-silenced *BDNF* v11 exon 2 contexts. The normalised *Renilla* luciferase levels recorded for these different plasmid constructs were then scaled to the normalised levels recorded for the plasmid construct containing the 5′ UTR of *BDNF* v11 wild-type.

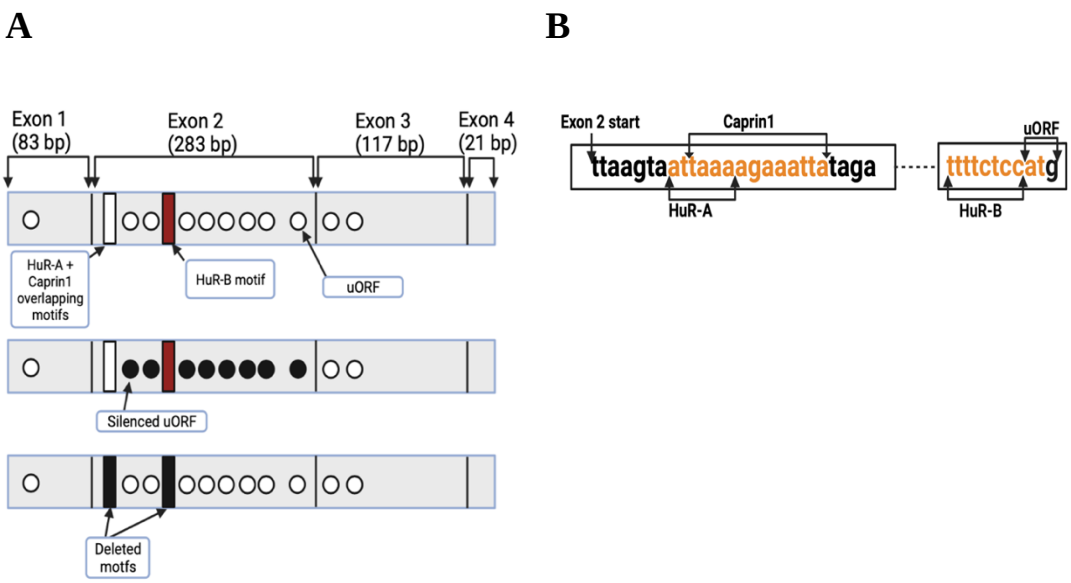


Figure 16- Examples of tested constructs containing a uORF-silenced *BDNF* v11 5′ UTR exon 2 and deletion of HuR and Caprin1 RNA-binding motifs.
(A), Representation of predicted uORFs and RNA-binding motifs in the 5′ UTR of *BDNF* transcript variant 11 (v11), and their respective silencing/deletions. uORFs are represented as white circles and silenced uORFs as black circles. uORF-silencing was carried out by converting adenine to thymine of uORF start codons. The white rectangle represents the predicted overlapping Human antigen R (HuR-A) and Cell cycle associated protein 1 (Caprin1) RNA-binding motifs, and the red rectangle represents the second predicted HuR (HuR-B) RNA-binding motif. Deleted RNA-binding motifs are shown as black rectangles. (B), An image showing the sequences of the predicted HuR-A and Caprin1 overlapping RNA-binding motifs and the HuR-B RNA-binding motif in exon 2 of *BDNF* v11. Nucleotides in orange show the predicted RNA-binding motif sequences in *BDNF* v11 5′ UTR exon 2 (from BRIO) and arrows in black show the deletions of the respective motifs that were performed in the tested constructs.

The deletion of any of these predicted RNA-binding motifs did not lead to any significant increases in luciferase activity, except for when all predicted motifs were deleted in the uORF-silenced context (Figure 17). However, this observed increase was probably mostly due to the protein upregulation effect of uORF-silencing rather than the binding of the respective proteins to the predicted RNA-binding motifs (since the observed increase was similar to that when the 8 uORFs were silenced). Therefore, these predicted RNA-binding motifs do not seem to be contributing to the translation repressive effect of exon 2.

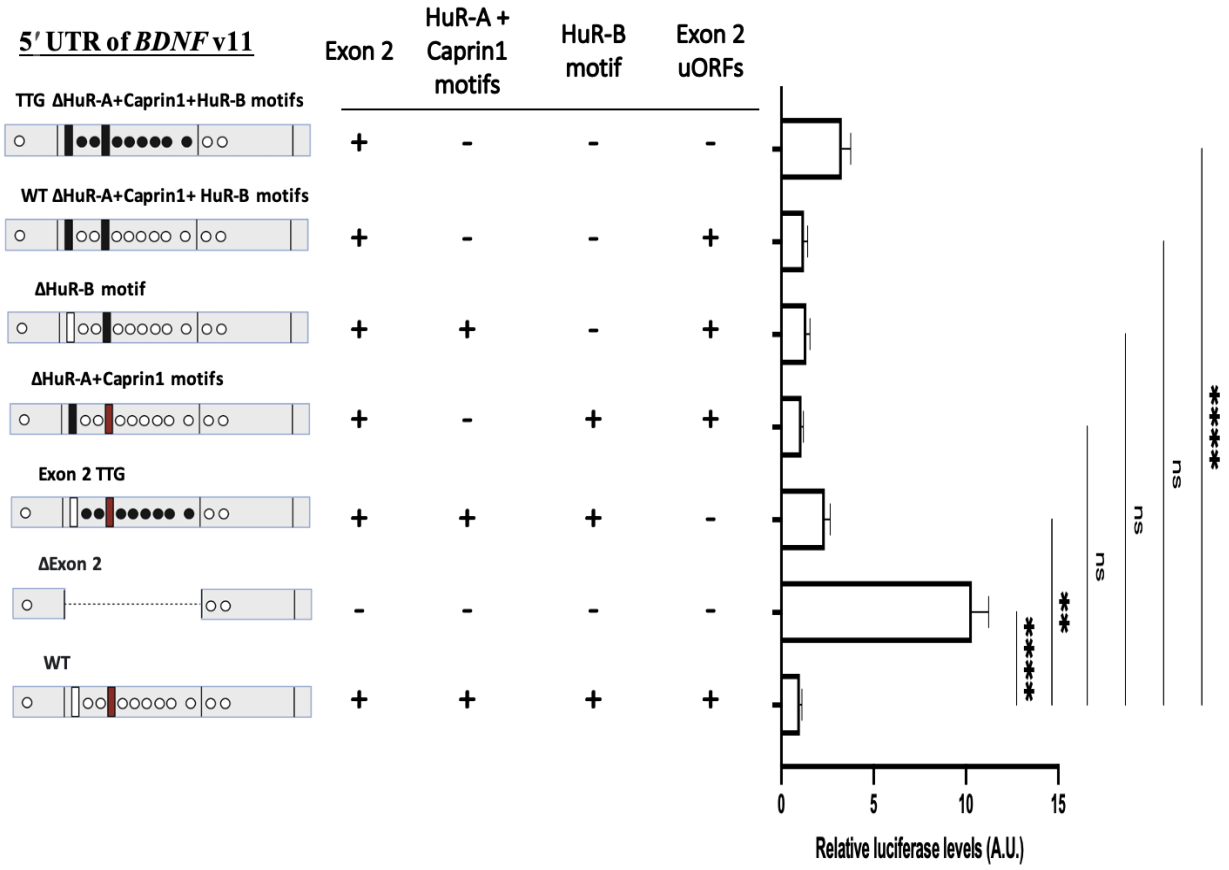


Figure 17- Silencing of uORFs, but not deletion of HuR or Caprin1 RNA-binding motifs in *BDNF* v11 5′ UTR exon 2, contributes to the increase in luciferase levels seen upon whole exon 2 deletion.

Bar chart showing the effects on relative luciferase levels upon deletion of predicted Human antigen R (HuR-A) and Cell cycle associated protein 1 (Caprin1) overlapping RNA-binding motifs, and deletion of an additional downstream HuR RNA-binding motif (HuR-B) individually (ΔHuR-A+Caprin1 motifs, ΔHuR-B motif), and in combination, in both the *BDNF* transcript variant 11 (v11) 5′ UTR exon 2 wild-type (WT ΔHuR-A+Caprin1+HuR-B motifs) and uORF-silenced contexts (TTG ΔHuR-A+Caprin1+HuR-B motifs). Constructs that contain deletion of *BDNF* v11 exon 2 (ΔExon 2) or silencing of uORFs in exon 2 (Exon 2 TTG) were also tested. The relevant *BDNF* v11 5′ UTR was inserted into a Dual-Luciferase reporter plasmid, HEK293T cells were transfected with constructs as indicated, and Dual-Luciferase reporter measurements performed 24 h later. The recorded *Renilla* luciferase levels for each tested construct were normalised to the corresponding Firefly luciferase levels. The normalised *Renilla* luciferase levels of all tested constructs were scaled to the normalised *Renilla* luciferase levels of *BDNF* v11 WT control. The layout of *BDNF* v11 5′ UTR exons in the tested constructs is shown, with a deleted exon represented as a dashed line and uORFs as white circles. The white rectangle represents HuR-A and Caprin1 overlapping RNA-binding motifs, and the red rectangle the HuR-B RNA-binding motif. Circles or rectangles in black represent the silencing or deletion of the uORF or motif/s, respectively. Statistical significance was tested by an ordinary one-way analysis of variance and *post hoc* multiple comparisons tests with Bonferroni correction. Values shown are means + SD, with 4 replicates per construct tested $^{**}P < 0.01$, $^{****}P < 0.0001$, ns = not significant.

To identify what region of *BDNF* v11 exon 2 may have contained translation repressive elements (in addition to uORFs), a deletion walk of exon 2 was performed (all exon 2 uORFs were silenced in these constructs to exclude uORF-associated effects). Specifically, 6 sequential deletions of 50 nucleotides (ΔSegment 6 had only 33 nucleotides deleted) were carried out in exon 2, which is 283 nucleotides long (Figure 18). Normalised *Renilla* luciferase levels of these sequential deletion constructs were scaled to the levels recorded for the plasmid construct containing the 5′ UTR of *BDNF* v11 when all 8 uORFs in exon 2 were silenced.

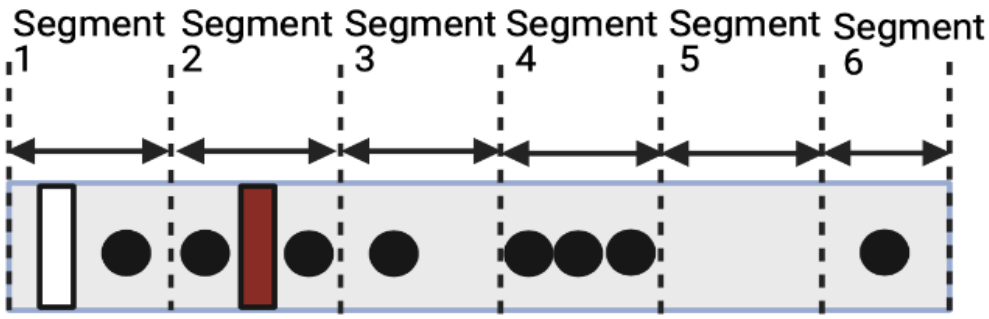


Figure 18- Sequential 50 nucleotide deletions of the 5′ UTR *BDNF* v11 exon 2 in the uORF-silenced context.
Exon 2 in the 5′ UTR of *BDNF* transcript variant 11 (v11) has 283 nucleotides. Six sequential deletions (ΔSegments 1-6) of 50 nucleotides (ΔSegment 6 had only 33 nucleotides deleted) were performed in exon 2. ΔSegment 1 has nucleotides 1-50 in exon 2 deleted, ΔSegment 2 has 51-100 deleted, ΔSegment 3 has 101-150 deleted, ΔSegment 4 has 151- 200 deleted, ΔSegment 5 has 201-250 deleted and ΔSegment 6 has 251-283 deleted. The black circles represent silenced uORFs. The white rectangle represents the predicted Human antigen R (HuR-A) and Cell cycle associated protein 1 (Caprin1) overlapping RNA-binding motifs, and the red rectangle represents an additional predicted HuR RNA-binding protein (HuR-B). All predicted motifs come from an RNA-binding motif search tool called BRIO.

Deletion of nucleotides 1-50 (Segment 1) and 51-100 (Segment 2) in uORF-silenced exon 2 of *BDNF* v11 5′ UTR led to significant increases in luciferase levels (Figure 19), with an especially large increase upon deletion of Segment 1. Sequential deletions of the remaining 183 nucleotides in exon 2 did not lead to significant increases in luciferase levels.

***BDNF* v11 uORF-silenced exon 2**

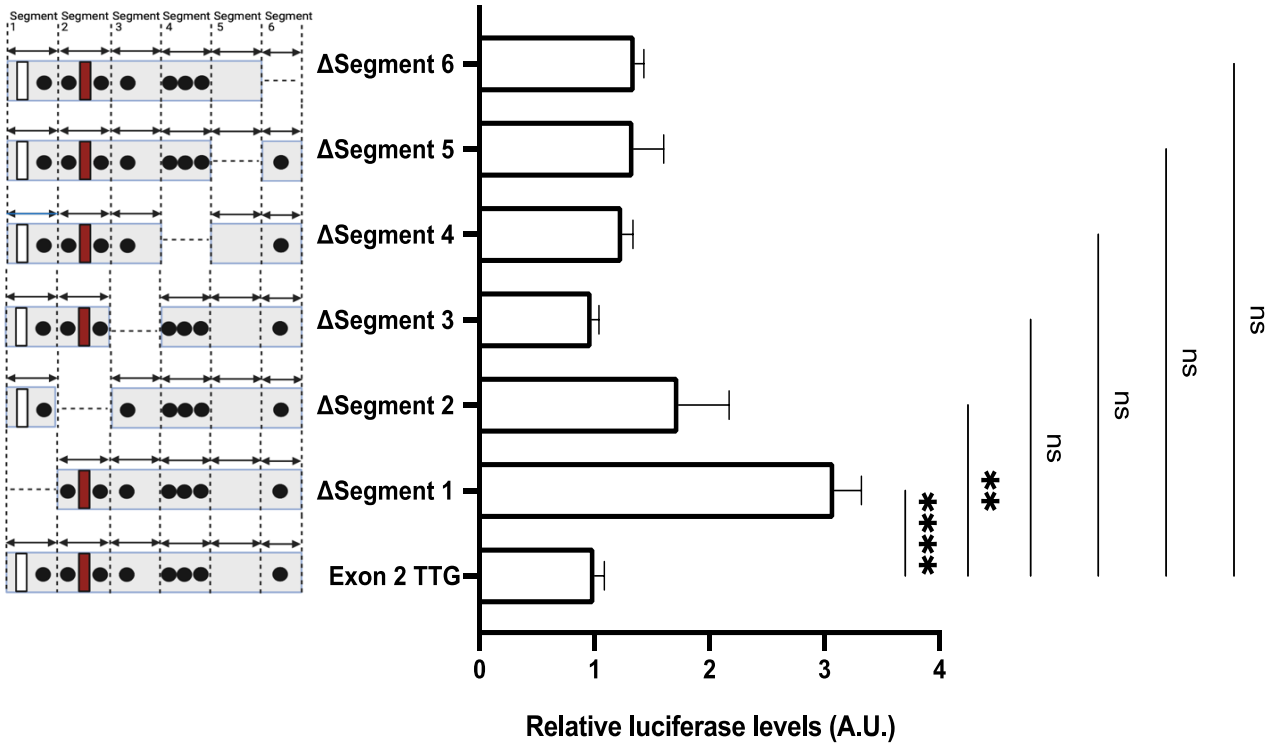


Figure 19- Deletion of nucleotides 1-50 and 51-100 in *BDNF* v11 5′ UTR exon 2 leads to a significant increase in luciferase levels.

Bar chart showing the effects on relative luciferase levels following sequential 50 nucleotide deletions (ΔSegments 1-6) in the 5′ UTR exon 2 of *BDNF* transcript variant 11 (v11) in the uORF-silenced context. ΔSegment 1 has exon 2 nucleotides 1-50 deleted, ΔSegment 2 has 51-100 deleted, ΔSegment 3 has 101-150 deleted, ΔSegment 4 has 151-200 deleted, ΔSegment 5 has 201-250 deleted and ΔSegment 6 has 251-283 deleted. The relevant *BDNF* v11 5′ UTR was inserted into a Dual-Luciferase reporter plasmid, HEK293T cells were transfected with constructs as indicated and Dual-Luciferase reporter measurements performed 24 h later. The recorded *Renilla* luciferase levels for each tested construct were normalised to the corresponding Firefly luciferase levels. The normalised *Renilla* luciferase levels of all tested constructs were scaled to the normalised *Renilla* luciferase levels of *BDNF* v11 exon 2 uORF-silenced (Exon 2 TTG) control. Silenced uORFs are shown as black circles, and deleted segments as dashed lines. The white rectangle represents the predicted Human antigen R (HuR-A) and Cell cycle associated protein 1 (Caprin1) overlapping RNA-binding motifs, and the red rectangle represents the second predicted HuR RNA-binding motif (HuR-B). Statistical significance was tested by an ordinary one-way analysis of variance and *post hoc* multiple comparisons tests with Bonferroni correction. Values shown are means + SD, with 4 replicates per construct tested. **P < 0.01, ****P < 0.0001, ns = not significant.

To analyse whether the increase in luciferase levels measured upon deletion of Segment 1 was similar to that observed when the whole of exon 2 was deleted, the normalised *Renilla* luciferase levels recorded after deletion of Segment 1 were re-scaled to those for the plasmid construct containing wild-type *BDNF* v11 5′ UTR. We realised that the increase in luciferase activity observed upon deletion of Segment 1 accounted for most of the increase recorded following deletion of the whole exon (Figure 20). Therefore, there seems to be at least 1 uORF-independent translation repressive element in the first 50 nucleotides of exon 2.

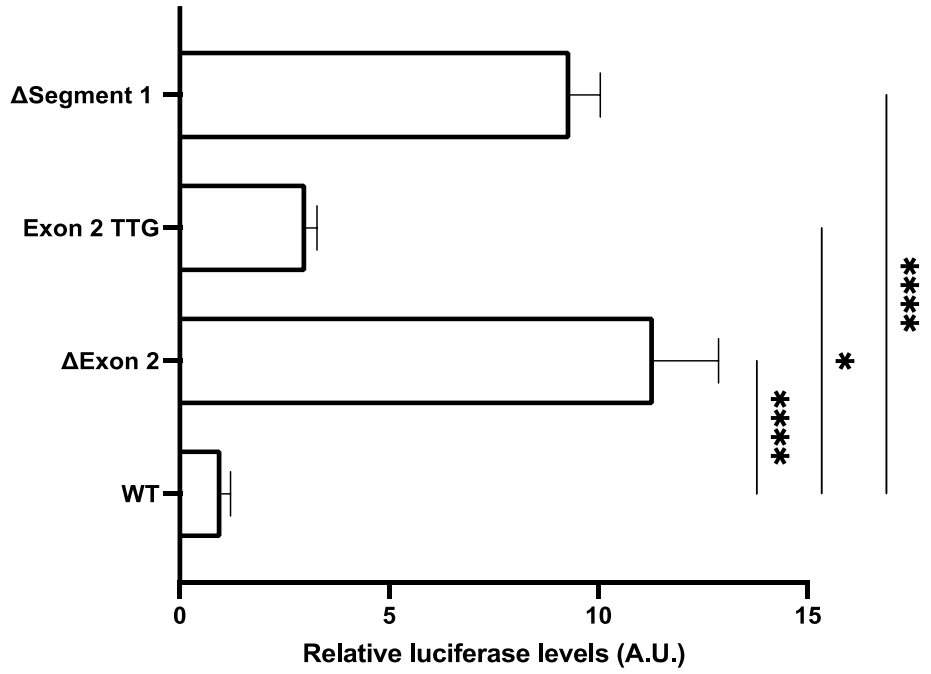


Figure 20- Deletion of the first 50 nucleotides in exon 2 of *BDNF* v11 5′ UTR accounts for most of the increase in luciferase levels recorded upon whole exon 2 deletion.

Bar chart showing the effect on relative luciferase levels when deleting the first 50 nucleotides (ΔSegment 1) in the 5′ UTR exon 2 of *BDNF* transcript variant 11 (v11) in the uORF-silenced context. The relative luciferase levels when the whole of exon 2 is skipped (ΔExon 2) or upon uORF-silencing in exon 2 (Exon 2 TTG) are also shown. The relevant *BDNF* v11 5′ UTR was inserted into a Dual-Luciferase reporter plasmid, HEK293T cells were transfected with constructs as indicated, and Dual-Luciferase reporter measurements performed 24 h later. The recorded *Renilla* luciferase levels for each tested construct were normalised to the corresponding Firefly luciferase levels. The normalised *Renilla* luciferase levels of the tested constructs were scaled to the normalised *Renilla* luciferase levels of *BDNF* v11 wild-type (WT) control. Statistical significance was tested by an ordinary one-way analysis of variance and *post hoc* multiple comparisons tests with Bonferroni correction. Values shown are means + SD, with 4 replicates per construct tested. **P* < 0.05, *****P* < 0.0001.

We hypothesised that the increase in luciferase activity seen upon deletion of the first 50 nucleotides in *BDNF* v11 5′ UTR exon 2 could be due to at least two factors; (i) deletion of a translation repressive RNA-binding motif within the first 50 nucleotides of exon 2, or (ii) a change in RNA secondary structure upon deletion of the first 50 nucleotides.

Further investigation using an RNA secondary structure predictor named RNAfold[127] led to the identification of a long hairpin which is present in the *BDNF* v11 5′ UTR following all 50 nucleotide sequential deletions in exon 2, except upon deletion of the first 50 nucleotides, where the hairpin is shorter. A short hairpin is also found following deletion of the whole of exon 2. The predicted long hairpin consisted of 91 nucleotides, with 64 nucleotides in exon 1 and 27 nucleotides in exon 2. While the short hairpin predicted in ΔSegment 1 (55 nucleotides) only consisted of nucleotides from exon 1 (Figure 21). We speculated that the presence of the long hairpin could be sterically blocking the ribosome from accessing the pORF and thus the presence of a shorter hairpin may enhance ribosomal translation of the pORF.

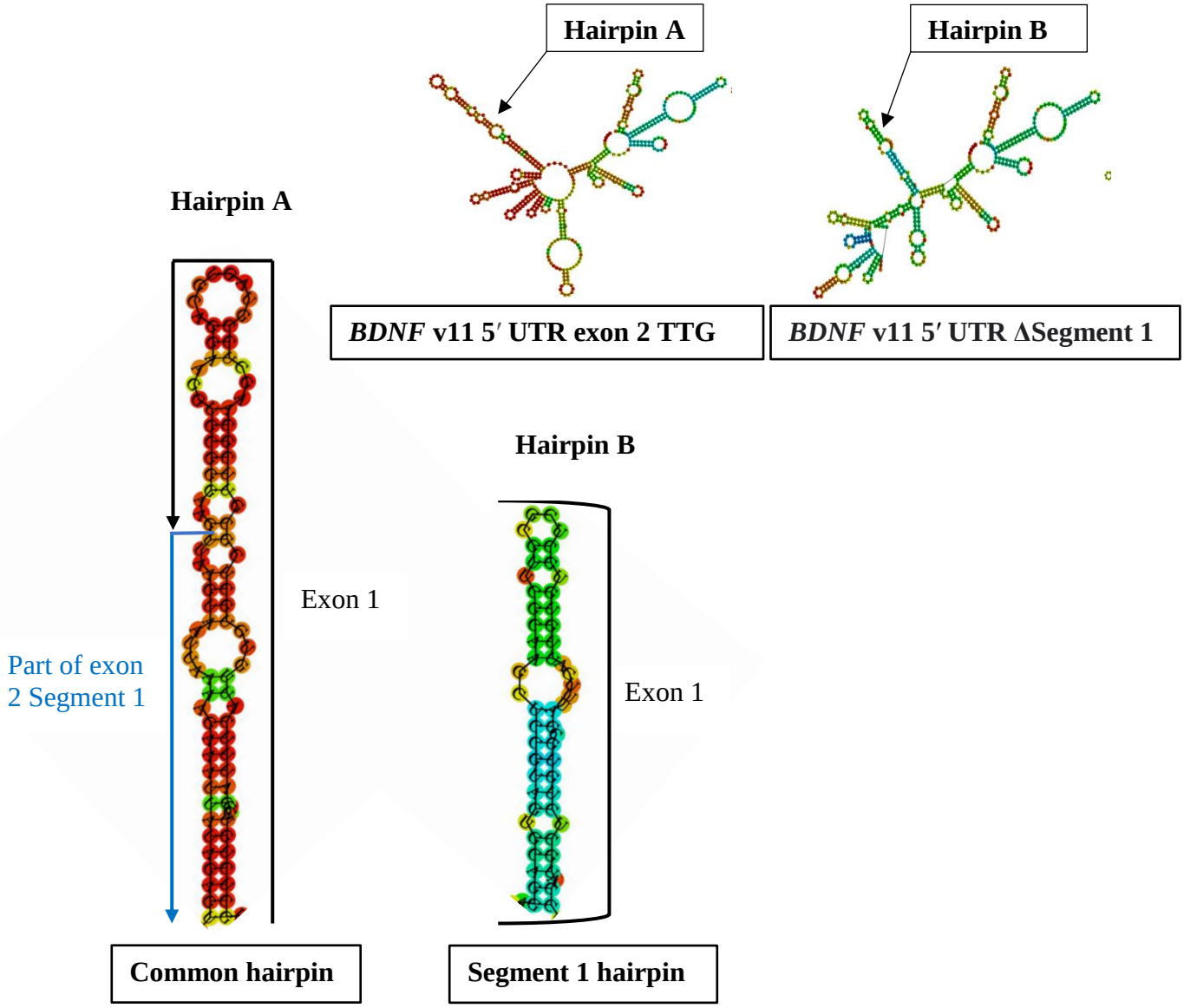


Figure 21- Predicted RNA secondary structure of the 5′ UTR of *BDNF* v11 following deletion of the first 50 nucleotides in exon 2.

The RNA structure predictor RNAfold predicts a common hairpin (Hairpin A) that has 91 nucleotides. Hairpin A is similar in both sequence and length in the predicted RNA secondary structures of the 5′ UTR of *BDNF* transcript variant 11 (v11) when exon 2 is wild-type, when exon 2 uORFs are silenced (exon 2 TTG), and in all 50 nucleotide sequential deletions in exon 2 (uORF-silenced context), except upon deletion of the first 50 nucleotides (ΔSegment 1). Hairpin A consists of 27 nucleotides from Segment 1 in exon 2 (Part of exon 2 Segment 1) and 64 nucleotides from exon 1. The predicted RNA secondary structure of *BDNF* v11 5′ UTR ΔSegment 1 has a shorter hairpin made up of 55 nucleotides found in exon 1 (ΔSegment 1 hairpin). The hairpin images shown are taken from RNAfold. A represents adenine, U represents uracil, C represents cytosine and G represents guanine.

To determine what the translation repressive element/s within the first 50 nucleotides of *BDNF* v11 exon 2 might be, we performed sequential deletions of 10 nucleotides in a uORF-silenced context and called them ΔSegment 1a, 1b, 1c, 1d and 1e (Figure 22).

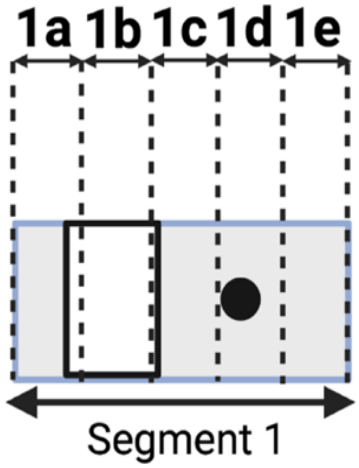


Figure 22- Sequential 10 nucleotide deletions within the first 50 nucleotides of *BDNF* v11 5′ UTR exon 2 in the uORF-silenced context.
A layout of the sequential 10 nucleotide deletions within the first 50 nucleotides (Segment 1) of *BDNF* transcript variant 11 (v11) 5′ UTR exon 2 in the uORF-silenced context is shown. Namely, ΔSegment 1a (1-10 deleted), ΔSegment 1b (11-20 deleted), ΔSegment 1c (21-30 deleted), ΔSegment 1d (31-40 deleted), ΔSegment 1e (41-50 deleted). The white rectangle represents the overlapping Human antigen receptor (HuR) and Cell cycle associated protein 1 (Caprin1) RNA-binding motifs, and the black circle represents a silenced uORF.

The normalised *Renilla* luciferase levels recorded for each 10 nucleotide deletion construct were scaled to the levels recorded for *BDNF* v11 when all 8 uORFs in exon 2 were silenced. However, no significant increases in luciferase levels were observed for any of the 10 nucleotide deletions (Figure 23).

The predicted RNA secondary structure of the *BDNF* v11 5′ UTR (uORF-silenced context) following deletion of Segment 1a in exon 2 contained a similar short hairpin as predicted for ΔSegment 1, and so we reasoned that if this short hairpin was a translation repressive element, then significant increases in luciferase levels should be observed for this construct, but none were found.

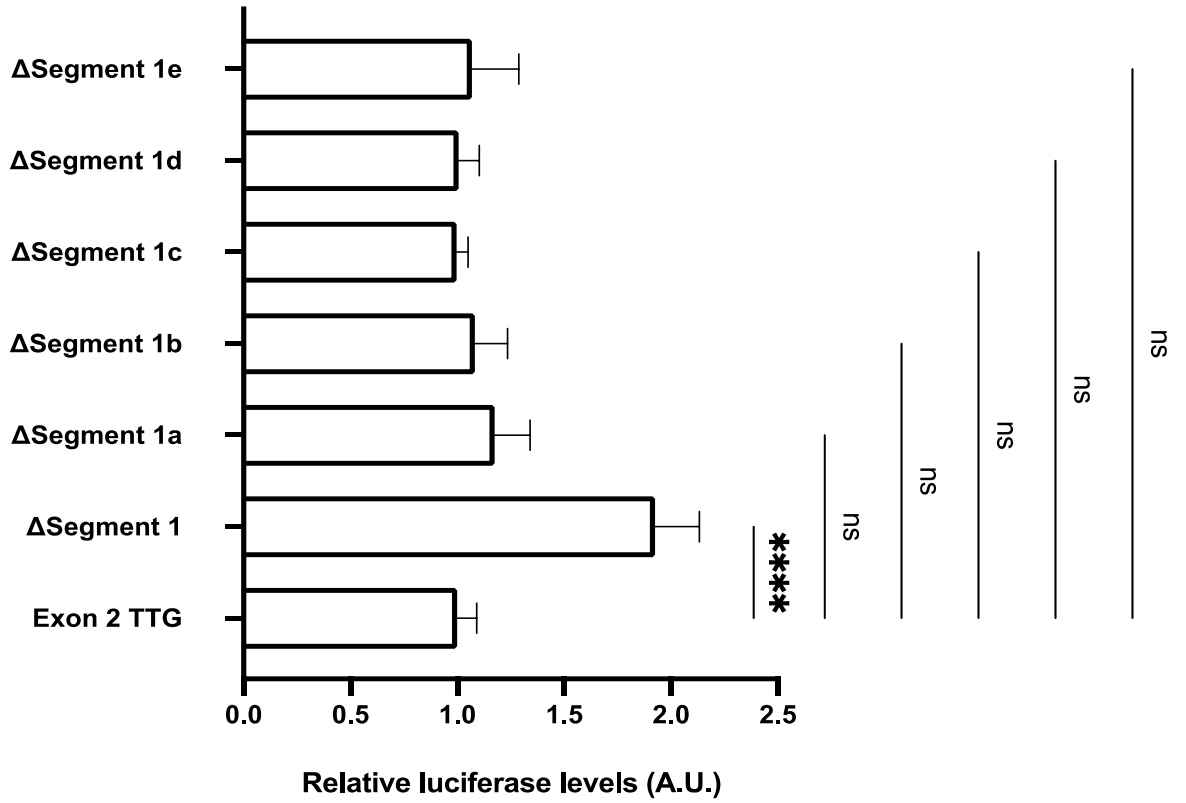


Figure 23- Sequential 10 nucleotide deletions in the first 50 nucleotides of *BDNF* v11 5′ UTR exon 2 causes no significant increases in luciferase levels.
Bar chart showing the effects on relative luciferase levels upon silencing of the uORFs (Exon 2 TTG) in the 5′ UTR exon 2 of *BDNF* transcript variant 11 (v11) and following deletion of the first 50 nucleotides of exon 2 in the in the uORF-silenced context (ΔSegment 1). The effects on relative luciferase levels following sequential 10 nucleotide deletions within the first 50 nucleotides of *BDNF* v11 exon 2 in the uORF-silenced context are also shown. Namely, ΔSegment 1a (1-10 deleted), ΔSegment 1b (11-20 deleted), ΔSegment 1c (21-30 deleted), ΔSegment 1d (31-40 deleted), ΔSegment 1e (41-50 deleted). The relevant *BDNF* v11 5′ UTR was inserted into a Dual-Luciferase reporter plasmid, HEK293T cells were transfected with constructs as indicated, and Dual-Luciferase reporter measurements performed 24 hours later. The recorded *Renilla* luciferase levels for each tested construct were normalised to the corresponding Firefly luciferase levels. The normalised *Renilla* luciferase levels of all tested constructs were scaled to the normalised *Renilla* luciferase levels of Exon 2 TTG control. Statistical significance was tested by an ordinary one-way analysis of variance and *post hoc* multiple comparisons tests with Bonferroni correction. Values shown are means + SD, with 4 replicates per construct tested. ****P < 0.0001, ns = not significant.

4 Discussion

Reduced levels of BDNF are associated with neurodegenerative, neurodevelopmental and psychiatric disorders. Hence, novel ways of upregulating BDNF levels are needed. Here, we sought to understand more about the repressive nature of uORFs in *BDNF* v5 and v14, in addition to examining whether the deletion of 5′ UTR uORF-containing exons in *BDNF* v11 and v14 could provide a way to increase protein levels.

We investigated the effects of silencing individual uORFs on luciferase levels. We showed that the 5 uORFs in *BDNF* v5 and the 3 uORFs in *BDNF* v14 have variable repressive potentials on protein translation. The significant increase in luciferase levels recorded upon silencing of the second uORF in *BDNF* v14 indicated that it has a strong repressive effect on pORF translation. In contrast, the silencing of individual uORFs in *BDNF* v5 did not lead to significant increases in luciferase levels.

We also studied the effects of silencing multiple uORFs. In general, the more uORFs were silenced, the greater the increases in luciferase levels were. Thus, the largest increases in luciferase levels recorded for *BDNF* v5 and v14 were when all uORFs were silenced. In particular, the second uORF in *BDNF* v14 was highly repressive, as the silencing of multiple uORFs in *BDNF* v14 only led to significant increases in luciferase levels when the second uORF was also silenced. These results support the idea that the silencing of repressive uORFs by steric block ASOs that mask uORF start codons or the editing of uORF start codons by ADAR enzymes may be effective ways of increasing protein levels.

In addition to examining the repressive potential of uORFs, we also investigated if deletion of uORF-containing exons could increase protein levels. The potential of exon skipping as a method for upregulating BDNF levels was evident, given the significant increases in luciferase levels observed upon deletion of *BDNF* v11 exon 2. However, the usefulness of this method needs to be determined for each exon within a given transcript variant, since no

significant increase in luciferase activity was recorded when *BDNF* v11 exon 3 was deleted, while a significant decrease in activity was observed upon deletion of exon 2 in *BDNF* v14. Interestingly, exon 2 of *BDNF* v14 could be useful in helping to identify translation promoting elements that could be targeted to reduce the expression of target proteins.

The masking of sequences that promote inclusion of *BDNF* v11 exon 2 (splice site sequences or ISE/ESEs) by steric block ASOs could provide a way for increasing the levels of BDNF. Moreover, the skipping of multiple exons could cause even greater increases in protein levels, since deletion of exons 2 and 3 in *BDNF* v11 led to a greater increase in luciferase activity than when these exons were deleted individually. However, the skipping of multiple exons as a therapy could have drawbacks, given the extent to which the 5′ UTR sequence is being altered in the process, and the use of multiple ASOs needed could render the treatment more toxic and expensive.

The 8 uORFs in *BDNF* v11 exon 2 contributed to the repression of pORF expression, but they did not fully account for the magnitude of increase seen upon deletion of the whole exon. Therefore, we investigated whether uORF-independent translation repressive elements could also play a role. Since HuR has previously been reported to promote uORF translation[128] and Caprin1 is involved in protein translation[129], we investigated if deletion of their predicted RNA-binding motifs in *BDNF* v11 exon 2 could be repressing translation of the pORF and/or contributing to the repressive nature of the uORFs. However, the (predicted) binding sites of these proteins did not seem to have any translation repressive effects, regardless of whether the uORFs were silenced.

Sequential deletions within *BDNF* v11 exon 2 helped to determine that deletion of the first 50 nucleotides and silencing of the 8 predicted uORFs in exon 2 accounted for most of the increase in luciferase levels observed upon deletion of the whole of exon 2. However, further sequential 10 nucleotide deletions within the first 50 nucleotides of exon 2 did not lead to

the identification of any translation repressive RNA-binding motifs or cause any apparent changes in (predicted) RNA secondary structure that could explain this increase. Although precise sequences with translation repressive effects could not be identified, it is likely that the reduced expression of the pORF was due to repression at the translational level rather than at the transcriptional level, given that no significant differences in mRNA levels were observed for any of the exon deletion constructs.

In the future, given that luciferase levels were measured here, it will be important to verify these results by examining whether the same effects are observed when looking at levels of endogenous BDNF, perhaps by designing steric block ASOs capable of skipping exon 2 of *BDNF* v11.

Moreover, it would be interesting to verify these results in other human cell lines. Larger deletions (greater than 10 nucleotides) within the first 50 nucleotides of *BDNF* v11 exon 2 could be performed to account for the possibility that there were multiple RNA-binding motifs that cooperated with each other, meaning that deletion of 10 nucleotides at a time did not fully remove their repressive effects. In addition, silencing of a non-canonical uORF start codon could be performed to investigate whether its translation repressive effect could be the reason for the increase in luciferase levels observed upon deletion of *BDNF* v11 exon 2[130]. Specifically, a GTG near-cognate start codon is found within a strong Kozak sequence context in the first 50 nucleotides of exon 2, but it should be noted that the efficacy of GTG as an alternative start codon has been questioned[131].

When designing ASO-mediated protein upregulation therapies, expression of the transcripts in the relevant target tissues should be considered. For example, it has been reported that *BDNF* v11 is not highly expressed in human brain hippocampus[40], which may limit its usefulness as a target for BDNF upregulation in this brain region that plays an important role in memory formation. Nevertheless, this work has highlighted the potential of skipping

uORF-containing exons for increasing BDNF levels, which could also be applied to other proteins.

In conclusion, this study has demonstrated that the silencing of individual and multiple uORFs within exons, as well as deletion of uORF-containing exons can upregulate luciferase levels. Further work is required to determine if ASO-mediated skipping of exon 2 in *BDNF* v11 leads to protein upregulation, and which elements within the first 50 nucleotides of *BDNF* v11 exon 2, in addition to uORFs, are mediating the repressive effect on pORF translation.

5 References

[1] Iacono M, Mignone F, Pesole G. uAUG and uORFs in human and rodent 5' untranslated mRNAs. Gene. 2005;349:97-105.

[2] Matsui M, Yachie N, Okada Y, Saito R, Tomita M. Bioinformatic analysis of post-transcriptional regulation by uORF in human and mouse. FEBS Letters. 2007;581:4184-8.

[3] Merrick WC and Pavitt GD. Protein synthesis initiation in eukaryotic cells. Cold Spring Harbor Perspectives in Biology. 2018;10:a033092.

[4] Jackson RJ, Hellen CU, Pestova TV. The mechanism of eukaryotic translation initiation and principles of its regulation. Nature Reviews Molecular Cell Biology. 2010;11:113-27.

[5] Cheung YN, Maag D, Mitchell SF, Fekete CA, Algire MA, Takacs JE, Shirokikh N, Pestova T, Lorsch JR, Hinnebusch AG. Dissociation of eIF1 from the 40S ribosomal subunit is a key step in start codon selection in vivo. Genes and Development. 2007;21:1217-30.

[6] Unbehaun A, Borukhov SI, Hellen CU, Pestova TV. Release of initiation factors from 48S complexes during ribosomal subunit joining and the link between establishment of codon-anticodon base-pairing and hydrolysis of eIF2-bound GTP. Genes and Development. 2004;18:3078-93.

[7] Maag D, Fekete CA, Gryczynski Z, Lorsch JR. A conformational change in the eukaryotic translation preinitiation complex and release of eIF1 signal recognition of the start codon. Molecular Cell. 2005;17:265-75.

[8] Pestova TV, Lomakin IB, Lee JH, Choi SK, Dever TE, Hellen CU. The joining of ribosomal subunits in eukaryotes requires eIF5B. Nature. 2000;403:332-5.

[9] Calvo SE, Pagliarini DJ, Mootha VK. Upstream open reading frames cause widespread reduction of protein expression and are polymorphic among humans. Proceedings of the National Academy of Sciences USA. 2009;106:7507-12.

[10] Wethmar K. The regulatory potential of upstream open reading frames in eukaryotic gene expression. Wiley Interdisciplinary Reviews: RNA. 2014;5:765-8.

[11] Kozak M. Compilation and analysis of sequences upstream from the translational start site in eukaryotic mRNAs. Nucleic Acids Research. 1984;12:857-72.

[12] Meijer HA and Thomas AA. Control of eukaryotic protein synthesis by upstream open reading frames in the 5′-untranslated region of an mRNA. Biochemical Journal. 2002;367:1-11.

[13] Ivanov IP, Saba JA, Fan CM, Wang J, Firth AE, Cao C, Green R, Dever TE. Evolutionarily conserved inhibitory uORFs sensitize Hox mRNA translation to start codon selection stringency. Proceedings of the National Academy of Sciences USA. 2022;119:e2117226119.

[14] Fijałkowska D, Verbruggen S, Ndah E, Jonckheere V, Menschaert G, Van Damme P. eIF1 modulates the recognition of suboptimal translation initiation sites and steers gene expression via uORFs. Nucleic Acids Research. 2017;45:7997-8013.

[15] Wilson DN, Arenz S, Beckmann R. Translation regulation via nascent polypeptide-mediated ribosome stalling. Current Opinion in Structural Biology. 2016;37:123-33.

[16] Hurt JA, Robertson AD, Burge CB. Global analyses of UPF1 binding and function reveal expanded scope of nonsense-mediated mRNA decay. Genome Research. 2013;23:1636-50.

[17] Gunišová S, Hronová V, Mohammad MP, Hinnebusch AG, Valášek LS. Please do not recycle! Translation reinitiation in microbes and higher eukaryotes. FEMS Microbiology Reviews. 2018;42:165-92.

[18] Kozak M. Constraints on reinitiation of translation in mammals. Nucleic Acids Research. 2001;29:5226-32.

[19] Morris DR and Geballe AP. Upstream open reading frames as regulators of mRNA translation. Molecular and Cellular Biology. 2000;20:8635-42.

[20] Chen J, Brunner AD, Cogan JZ, Nuñez JK, Fields AP, Adamson B, Itzhak DN, Li JY, Mann M, Leonetti MD, Weissman JS. Pervasive functional translation of noncanonical human open reading frames. Science. 2020;367:1140-6.

[21] Samandi S, Roy AV, Delcourt V, Lucier JF, Gagnon J, Beaudoin MC, Vanderperre B, Breton MA, Motard J, Jacques JF, Brunelle M. Deep transcriptome annotation enables the discovery and functional characterization of cryptic small proteins. ELife. 2017;6:e27860.

[22] Liu J, Yosten GL, Ji H, Zhang D, Zheng W, Speth RC, Samson WK, Sandberg K. Selective inhibition of angiotensin receptor signaling through Erk1/2 pathway by a novel peptide. American Journal of Physiology - Regulatory, Integrative and Comparative Physiology. 2014;306:619-26.

[23] Lee CF, Lai HL, Lee YC, Chien CL, Chern Y. The A2A adenosine receptor is a dual coding gene: a novel mechanism of gene usage and signal transduction. Journal of Biological Chemistry. 2014;289:1257-70.

[24] Jayaram DR, Frost S, Argov C, Liju VB, Anto NP, Muraleedharan A, Ben-Ari A, Sinay R, Smoly I, Novoplansky O, Isakov N. Unraveling the hidden role of a uORF-encoded peptide as a kinase inhibitor of PKCs. Proceedings of the National Academy of Sciences USA. 2021;118:e2018899118.

[25] Young SK and Wek RC. Upstream open reading frames differentially regulate gene-specific translation in the integrated stress response. Journal of Biological Chemistry. 2016;291:16927-35.

[26] Vattem KM and Wek RC. Reinitiation involving upstream ORFs regulates ATF4 mRNA translation in mammalian cells. Proceedings of the National Academy of Sciences USA. 2004;101:11269-74.

[27] Werner M, Feller A, Messenguy F, Piérard A. The leader peptide of yeast gene CPA1 is essential for the translational repression of its expression. Cell. 1987;49:805-13.

[28] Gaba A, Jacobson A, Sachs MS. Ribosome occupancy of the yeast CPA1 upstream open reading frame termination codon modulates nonsense-mediated mRNA decay. Molecular Cell. 2005;20:449-60.

[29] Wethmar K, Schulz J, Muro EM, Talyan S, Andrade-Navarro MA, Leutz A. Comprehensive translational control of tyrosine kinase expression by upstream open reading frames. Oncogene. 2016;35:1736-42.

[30] Neafsey DE and Galagan JE. Dual modes of natural selection on upstream open reading frames. Molecular Biology and Evolution. 2007;24:1744-51.

[31] Whiffin N, Karczewski KJ, Zhang X, Chothani S, Smith MJ, Evans DG, Roberts AM, Quaife NM, Schafer S, Rackham O, Alföldi J. Characterising the loss-of-function impact of 5'untranslated region variants in 15,708 individuals. Nature Communications. 2020;11:1-2.

[32] McGillivray P, Ault R, Pawashe M, Kitchen R, Balasubramanian S, Gerstein M. A comprehensive catalog of predicted functional upstream open reading frames in humans. Nucleic Acids Research. 2018;46:3326-38.

[33] Barbosa C, Peixeiro I, Romão L. Gene expression regulation by upstream open reading frames and human disease. PLOS Genetics. 2013;9:e1003529.

[34] Liu L, Dilworth D, Gao L, Monzon J, Summers A, Lassam N, Hogg D. Mutation of the CDKN2A 5'UTR creates an aberrant initiation codon and predisposes to melanoma. Nature Genetics. 1999;21:128-32.

[35] Lukowski SW, Bombieri C, Trezise AE. Disrupted posttranscriptional regulation of the cystic fibrosis transmembrane conductance regulator (CFTR) by a 5′ UTR mutation is associated with a cftr-related disease. Human Mutation. 2011;32:e2266-82.

[36] Occhi G, Regazzo D, Trivellin G, Boaretto F, Ciato D, Bobisse S, Ferasin S, Cetani F, Pardi E, Korbonits M, Pellegata NS. A novel mutation in the upstream open reading frame of the CDKN1B gene causes a MEN4 phenotype. PLOS Genetics. 2013;9:e1003350.

[37] Ghilardi N, Wiestner A, Kikuchi M, Ohsaka A, Skoda RC. Hereditary thrombocythaemia in a Japanese family is caused by a novel point mutation in the thrombopoietin gene. British Journal of Haematology. 1999;107:310-6.

[38] Cazzola M and Skoda RC. Translational pathophysiology: a novel molecular mechanism of human disease. Blood. 2000;95:3280-8.

[39] Pruunsild P, Kazantseva A, Aid T, Palm K, Timmusk T. Dissecting the human BDNF locus: bidirectional transcription, complex splicing, and multiple promoters. Genomics. 2007;90:397-406.

[40] Cattaneo A, Cattane N, Begni V, Pariante CM, Riva MA. The human BDNF gene: peripheral gene expression and protein levels as biomarkers for psychiatric disorders. Translational Psychiatry. 2016;6:e958.

[41] Mowla SJ, Pareek S, Farhadi HF, Petrecca K, Fawcett JP, Seidah NG, Morris SJ, Sossin WS, Murphy RA. Differential sorting of nerve growth factor and brain-derived neurotrophic factor in hippocampal neurons. Journal of Neuroscience. 1999;19:2069-80.

[42] Seidah NG, Benjannet S, Pareek S, Chrétien M, Murphy RA. Cellular processing of the neurotrophin precursors of NT3 and BDNF by the mammalian proprotein convertases. FEBS Letters. 1996;379:247-50.

[43] Mowla SJ, Farhadi HF, Pareek S, Atwal JK, Morris SJ, Seidah NG, Murphy RA. Biosynthesis and post-translational processing of the precursor to brain-derived neurotrophic factor. Journal of Biological Chemistry. 2001;276:12660-6.

[44] Lee R, Kermani P, Teng KK, Hempstead BL. Regulation of cell survival by secreted proneurotrophins. Science. 2001;294:1945-8.

[45] Matsumoto T, Rauskolb S, Polack M, Klose J, Kolbeck R, Korte M, Barde YA. Biosynthesis and processing of endogenous BDNF: CNS neurons store and secrete BDNF, not pro-BDNF. Nature Neuroscience. 2008;11:131-3.

[46] Soppet D, Escandon E, Maragos J, Middlemas DS, Raid SW, Blair J, Burton LE, Stanton BR, Kaplan DR, Hunter T, Nikolics K. The neurotrophic factors brain-derived neurotrophic factor and neurotrophin-3 are ligands for the trkB tyrosine kinase receptor. Cell. 1991;65:895-903.

[47] Nikoletopoulou V, Lickert H, Frade JM, Rencurel C, Giallonardo P, Zhang L, Bibel M, Barde YA. Neurotrophin receptors TrkA and TrkC cause neuronal death whereas TrkB does not. Nature. 2010;467:59-63.

[48] Tanaka JI, Horiike Y, Matsuzaki M, Miyazaki T, Ellis-Davies GC, Kasai H. Protein synthesis and neurotrophin-dependent structural plasticity of single dendritic spines. Science. 2008;319:1683-7.

[49] Horch HW and Katz LC. BDNF release from single cells elicits local dendritic growth in nearby neurons. Nature Neuroscience. 2002;5:1177-84.

[50] Figurov A, Pozzo-Miller LD, Olafsson P, Wang T, Lu B. Regulation of synaptic responses to high-frequency stimulation and LTP by neurotrophins in the hippocampus. Nature. 1996;381:706-9.

[51] Kang H and Schuman EM. Long-lasting neurotrophin-induced enhancement of synaptic transmission in the adult hippocampus. Science. 1995;267:1658-62.

[52] Egan MF, Kojima M, Callicott JH, Goldberg TE, Kolachana BS, Bertolino A, Zaitsev E, Gold B, Goldman D, Dean M, Lu B. The BDNF val66met polymorphism affects activity-dependent secretion of BDNF and human memory and hippocampal function. Cell. 2003;112:257-69.

[53] Michalski B and Fahnestock M. Pro-brain-derived neurotrophic factor is decreased in parietal cortex in Alzheimer's disease. Molecular Brain Research. 2003;111:148-54.

[54] Peng S, Wuu J, Mufson EJ, Fahnestock M. Precursor form of brain-derived neurotrophic factor and mature brain-derived neurotrophic factor are decreased in the pre-clinical stages of Alzheimer's disease. Journal of Neurochemistry. 2005;93:1412-21.

[55] Mogi M, Togari A, Kondo T, Mizuno Y, Komure O, Kuno S, Ichinose H, Nagatsu T. Brain-derived growth factor and nerve growth factor concentrations are decreased in the substantia nigra in Parkinson's disease. Neuroscience Letters. 1999;270:45-8.

[56] Parain K, Murer MG, Yan Q, Faucheux B, Agid Y, Hirsch E, Raisman-Vozari R. Reduced expression of brain-derived neurotrophic factor protein in Parkinson's disease substantia nigra. NeuroReport. 1999;10:557-61.

[57] Strand AD, Baquet ZC, Aragaki AK, Holmans P, Yang L, Cleren C, Beal MF, Jones L, Kooperberg C, Olson JM, Jones KR. Expression profiling of Huntington's disease models suggests that brain-derived neurotrophic factor depletion plays a major role in striatal degeneration. Journal of Neuroscience. 2007;27:11758-68.

[58] Zuccato C, Ciammola A, Rigamonti D, Leavitt BR, Goffredo D, Conti L, MacDonald ME, Friedlander RM, Silani V, Hayden MR, Timmusk T. Loss of huntingtin-mediated BDNF gene transcription in Huntington's disease. Science. 2001;293:493-8.

[59] Dwivedi Y, Rizavi HS, Conley RR, Roberts RC, Tamminga CA, Pandey GN. Altered gene expression of brain-derived neurotrophic factor and receptor tyrosine kinase B in postmortem brain of suicide subjects. Archives of General Psychiatry. 2003;60:804-15.

[60] Molendijk ML, Spinhoven P, Polak M, Bus BA, Penninx BW, Elzinga BM. Serum BDNF concentrations as peripheral manifestations of depression: evidence from a systematic review and meta-analyses on 179 associations (N= 9484). Molecular Psychiatry. 2014;19:791-800.

[61] Kim HJ, Bayarsaikhan D, Lee J, Bayarsaikhan G, Lee B. Brain-Derived Neurotrophic Factor Secreting Human Mesenchymal Stem Cells Improve Outcomes in Rett Syndrome Mouse Models. Frontiers in Neuroscience. 2021;15:725398.

[62] Nagahara AH, Merrill DA, Coppola G, Tsukada S, Schroeder BE, Shaked GM, Wang L, Blesch A, Kim A, Conner JM, Rockenstein E. Neuroprotective effects of brain-derived neurotrophic factor in rodent and primate models of Alzheimer's disease. Nature Medicine. 2009;15:331-7.

[63] Levivier M, Przedborski S, Bencsics C, Kang UJ. Intrastriatal implantation of fibroblasts genetically engineered to produce brain-derived neurotrophic factor prevents degeneration of dopaminergic neurons in a rat model of Parkinson's disease. Journal of Neuroscience. 1995;15:7810-20.

[64] Frim DM, Uhler TA, Galpern WR, Beal MF, Breakefield XO, Isacson O. Implanted fibroblasts genetically engineered to produce brain-derived neurotrophic factor prevent 1-methyl-4-phenylpyridinium toxicity to dopaminergic neurons in the rat. Proceedings of the National Academy of Sciences USA. 1994;91:5104-8.

[65] Simmons DA, Rex CS, Palmer L, Pandyarajan V, Fedulov V, Gall CM, Lynch G. Up-regulating BDNF with an ampakine rescues synaptic plasticity and memory in Huntington's disease knockin mice. Proceedings of the National Academy of Sciences USA. 2009;106:4906-11.

[66] Ferrer I, Ballabriga J, Martí E, Pérez E, Alberch J, Arenas E. BDNF up-regulates TrkB protein and prevents the death of CA1 neurons following transient forebrain ischemia. Brain Pathology.1998;8:253-61.

[67] Blesch A and Tuszynski MH. Transient growth factor delivery sustains regenerated axons after spinal cord injury. Journal of Neuroscience. 2007;27:10535-45.

[68] Miranda M, Morici JF, Zanoni MB, Bekinschtein P. Brain-derived neurotrophic factor: a key molecule for memory in the healthy and the pathological brain. Frontiers in Cellular Neuroscience. 2019;13:363.

[69] Nagahara AH and Tuszynski MH. Potential therapeutic uses of BDNF in neurological and psychiatric disorders. Nature Reviews Drug Discovery. 2011;10:209-19.

[70] O'Leary PD and Hughes RA. Design of potent peptide mimetics of brain-derived neurotrophic factor. Journal of Biological Chemistry. 2003;278:25738-44.

[71] Wurzelmann M, Romeika J, Sun D. Therapeutic potential of brain-derived neurotrophic factor (BDNF) and a small molecular mimics of BDNF for traumatic brain injury. Neural Regeneration Research. 2017;12:7-12.

[72] Garcia LS, Comim CM, Valvassori SS, Réus GZ, Barbosa LM, Andreazza AC, Stertz L, Fries GR, Gavioli EC, Kapczinski F, Quevedo J. Acute administration of ketamine induces antidepressant-like effects in the forced swimming test and increases BDNF levels in the rat hippocampus. Progress in Neuro-Psychopharmacology and Biological Psychiatry. 2008;32:140-4.

[73] Drzyzga ŁR, Marcinowska A, Obuchowicz E. Antiapoptotic and neurotrophic effects of antidepressants: a review of clinical and experimental studies. Brain Research Bulletin. 2009;79:248-57.

[74] Leyhe T, Eschweiler GW, Stransky E, Gasser T, Annas P, Basun H, Laske C. Increase of BDNF serum concentration in lithium treated patients with early Alzheimer's disease. Journal of Alzheimer's Disease. 2009;16:649-56.

[75] de Sousa RT, van de Bilt MT, Diniz BS, Ladeira RB, Portela LV, Souza DO, Forlenza OV, Gattaz WF, Machado-Vieira R. Lithium increases plasma brain-derived neurotrophic factor in acute bipolar mania: a preliminary 4-week study. Neuroscience Letters. 2011;494:54-6.

[76] A Clinical Trial of AAV2-BDNF Gene Therapy in Early Alzheimer's Disease and Mild Cognitive Impairment | ClinicalTrials.gov [Internet]. [cited 2022 July 13]; Available at: https://clinicaltrials.gov/ct2/show/NCT05040217

[77] Modarresi F, Faghihi MA, Lopez-Toledano MA, Fatemi RP, Magistri M, Brothers SP, van der Brug MP, Wahlestedt C. Natural antisense inhibition results in transcriptional de-repression and gene upregulation. Nature Biotechnology. 2012;30:453-59.

[78] Kole R, Krainer AR, Altman S. RNA therapeutics: beyond RNA interference and antisense oligonucleotides. Nature Reviews Drug Discovery. 2012;11:125-40.

[79] Scharner J, Ma WK, Zhang Q, Lin KT, Rigo F, Bennett CF, Krainer AR. Hybridization-mediated off-target effects of splice-switching antisense oligonucleotides. Nucleic Acids Research. 2020;48:802-16.

[80] Chen M and Manley JL. Mechanisms of alternative splicing regulation: insights from molecular and genomics approaches. Nature Reviews Molecular Cell Biology. 2009;10:741-54.

[81] Dominski Z and Kole R. Restoration of correct splicing in thalassemic pre-mRNA by antisense oligonucleotides. Proceedings of the National Academy of Sciences USA. 1993;90:8673-7.

[82] Bladen CL, Salgado D, Monges S, Foncuberta ME, Kekou K, Kosma K, Dawkins H, Lamont L, Roy AJ, Chamova T, Guergueltcheva V. The TREAT-NMD DMD Global Database: analysis of more than 7,000 Duchenne muscular dystrophy mutations. Human Mutation. 2015;36:395-402.

[83] Aartsma-Rus A, Janson AA, Kaman WE, Bremmer-Bout M, van Ommen GJ, den Dunnen JT, van Deutekom JC. Antisense-induced multiexon skipping for Duchenne muscular dystrophy makes more sense. The American Journal of Human Genetics. 2004;74:83-92.

[84] Kim YJ, Sivetz N, Layne J, Voss DM, Yang L, Zhang Q, Krainer AR. Exon-skipping antisense oligonucleotides for cystic fibrosis therapy. Proceedings of the National Academy of Sciences USA. 2022;119:e2114858118.

[85] Ward AJ, Norrbom M, Chun S, Bennett CF, Rigo F. Nonsense-mediated decay as a terminating mechanism for antisense oligonucleotides. Nucleic Acids Research. 2014;42:5871-9.

[86] Lefebvre S, Bürglen L, Reboullet S, Clermont O, Burlet P, Viollet L, Benichou B, Cruaud C, Millasseau P, Zeviani M, Le Paslier D. Identification and characterization of a spinal muscular atrophy-determining gene. Cell. 1995;80:155-65.

[87] Lorson CL, Hahnen E, Androphy EJ, Wirth B. A single nucleotide in the SMN gene regulates splicing and is responsible for spinal muscular atrophy. Proceedings of the National Academy of Sciences USA. 1999;96:6307-11.

[88] Monani UR, Lorson CL, Parsons DW, Prior TW, Androphy EJ, Burghes AH, McPherson JD. A single nucleotide difference that alters splicing patterns distinguishes the SMA gene SMN1 from the copy gene SMN2. Human Molecular Genetics. 1999;8:1177-83.

[89] Cartegni L and Krainer AR. Disruption of an SF2/ASF-dependent exonic splicing enhancer in SMN2 causes spinal muscular atrophy in the absence of SMN1. Nature Genetics. 2002;30:377-84.

[90] Hua Y, Sahashi K, Hung G, Rigo F, Passini MA, Bennett CF, Krainer AR. Antisense correction of SMN2 splicing in the CNS rescues necrosis in a type III SMA mouse model. Genes and Development. 2010;24:1634-44.

[91] Corey DR. Nusinersen, an antisense oligonucleotide drug for spinal muscular atrophy. Nature Neuroscience. 2017;20:497-9.

[92] Li Q. Nusinersen as a therapeutic agent for spinal muscular atrophy. Yonsei Medical Journal. 2020;61:273-83.

[93] Baker BF, Lot SS, Condon TP, Cheng-Flournoy S, Lesnik EA, Sasmor HM, Bennett CF. 2′-O-(2-Methoxy) ethyl-modified anti-intercellular adhesion molecule 1 (ICAM-1) oligonucleotides selectively increase the ICAM-1 mRNA level and inhibit formation of the ICAM-1 translation initiation complex in human umbilical vein endothelial cells. Journal of Biological Chemistry. 1997;272:11994-12000.

[94] Vickers TA, Wyatt JR, Burckin T, Bennett CF, Freier SM. Fully modified 2′ MOE oligonucleotides redirect polyadenylation. Nucleic Acids Research. 2001;29:1293-9.

[95] Liang XH, Shen W, Sun H, Migawa MT, Vickers TA, Crooke ST. Translation efficiency of mRNAs is increased by antisense oligonucleotides targeting upstream open reading frames. Nature Biotechnology. 2016;34:875-80.

[96] Merkle T, Merz S, Reautschnig P, Blaha A, Li Q, Vogel P, Wettengel J, Li JB, Stafforst T. Precise RNA editing by recruiting endogenous ADARs with antisense oligonucleotides. Nature Biotechnology. 2019;37:133-8.

[97] Paunovska K, Loughrey D, Dahlman JE. Drug delivery systems for RNA therapeutics. Nature Reviews Genetics. 2022;23:265-80.

[98] Crooke ST, Vickers TA, Liang XH. Phosphorothioate modified oligonucleotide–protein interactions. Nucleic Acids Research. 2020;48:5235-53.

[99] Weidner DA, Valdez BC, Henning D, Greenberg S, Busch H. Phosphorothioate oligonucleotides bind in a non sequence-specific manner to the nucleolar protein C23/nucleolin. FEBS Letters. 1995;366:146-50.

[100] Liang XH, Shen W, Sun H, Prakash TP, Crooke ST. TCP1 complex proteins interact with phosphorothioate oligonucleotides and can co-localize in oligonucleotide-induced nuclear bodies in mammalian cells. Nucleic Acids Research. 2014;42:7819-32.

[101] Iwamoto N, Butler DC, Svrzikapa N, Mohapatra S, Zlatev I, Sah DW, Standley SM, Lu G, Apponi LH, Frank-Kamenetsky M, Zhang JJ. Control of phosphorothioate stereochemistry substantially increases the efficacy of antisense oligonucleotides. Nature Biotechnology. 2017;35:845-51.

[102] Shen X and Corey DR. Chemistry, mechanism and clinical status of antisense oligonucleotides and duplex RNAs. Nucleic Acids Research. 2018;46:1584-600.

[103] Kulkarni JA, Witzigmann D, Thomson SB, Chen S, Leavitt BR, Cullis PR, van der Meel R. The current landscape of nucleic acid therapeutics. Nature Nanotechnology. 2021;16:630-43.

[104] Vester B and Wengel J. LNA (locked nucleic acid): high-affinity targeting of complementary RNA and DNA. Biochemistry. 2004;43:13233-41.

[105] Renneberg D and Leumann CJ. Watson-Crick base-pairing properties of tricyclo-DNA. Journal of the American Chemical Society. 2002;124:5993-6002.

[106] Hammond SM, Aartsma-Rus A, Alves S, Borgos SE, Buijsen RA, Collin RW, Covello G, Denti MA, Desviat LR, Echevarría L, Foged C. Delivery of oligonucleotide-based therapeutics: challenges and opportunities. EMBO Molecular Medicine. 2021;13:e13243.

[107] Quemener AM, Centomo ML, Sax SL, Panella R. Small drugs, huge impact: The extraordinary impact of antisense oligonucleotides in research and drug development. Molecules. 2022;27:536.

[108] Roberts TC, Langer R, Wood MJ. Advances in oligonucleotide drug delivery. Nature Reviews Drug Discovery. 2020;19:673-94.

[109] Seth PP, Tanowitz M, Bennett CF. Selective tissue targeting of synthetic nucleic acid drugs. The Journal of Clinical Investigation. 2019;129:915-25.

[110] Gagliardi M and Ashizawa AT. The challenges and strategies of antisense oligonucleotide drug delivery. Biomedicines. 2021;9:433.

[111] Lee RT, Lin P, Lee YC. New synthetic cluster ligands for galactose/N-acetylgalactosamine-specific lectin of mammalian liver. Biochemistry.1984;23:4255-61.

[112] Prakash TP, Graham MJ, Yu J, Carty R, Low A, Chappell A, Schmidt K, Zhao C, Aghajan M, Murray HF, Riney S. Targeted delivery of antisense oligonucleotides to hepatocytes using triantennary N-acetyl galactosamine improves potency 10-fold in mice. Nucleic Acids Research. 2014;42:8796-807.

[113] Debacker AJ, Voutila J, Catley M, Blakey D, Habib N. Delivery of oligonucleotides to the liver with GalNAc: from research to registered therapeutic drug. Molecular Therapy. 2020;28:1759-71.

[114] Dugal-Tessier J, Thirumalairajan S, Jain N. Antibody-oligonucleotide conjugates: a twist to antibody-drug conjugates. Journal of Clinical Medicine. 2021;10:838.

[115] White RR, Sullenger BA, Rusconi CP. Developing aptamers into therapeutics. The Journal of Clinical Investigation. 2000;106:929-34.

[116] Tenchov R, Bird R, Curtze AE, Zhou Q. Lipid Nanoparticles─ From Liposomes to mRNA Vaccine Delivery, a Landscape of Research Diversity and Advancement. ACS Nano. 2021;15:16982-17015.

[117] Nag OK and Awasthi V. Surface engineering of liposomes for stealth behavior. Pharmaceutics. 2013;5:542-69.

[118] Wang X, Ishida T, Kiwada H. Anti-PEG IgM elicited by injection of liposomes is involved in the enhanced blood clearance of a subsequent dose of PEGylated liposomes. Journal of Controlled Release. 2007;119:236-44.

[119] Hoang Thi TT, Pilkington EH, Nguyen DH, Lee JS, Park KD, Truong NP. The importance of poly (ethylene glycol) alternatives for overcoming PEG immunogenicity in drug delivery and bioconjugation. Polymers. 2020;12:298.

[120] Jiang S, Ge Z, Mou S, Yan H, Fan C. Designer DNA nanostructures for therapeutics. Chem. 2021;7:1156-79.

[121] Alvarez-Erviti L, Seow Y, Yin H, Betts C, Lakhal S, Wood MJ. Delivery of siRNA to the mouse brain by systemic injection of targeted exosomes. Nature Biotechnology. 2011;29:341-5.

[122] Wang J, Chen D, Ho EA. Challenges in the development and establishment of exosome-based drug delivery systems. Journal of Controlled Release. 2021;329:894-906.

[123] Pfaffl MW. A new mathematical model for relative quantification in real-time RT–PCR. Nucleic Acids Research. 2001;29:e45.

[124] Kent WJ, Sugnet CW, Furey TS, Roskin KM, Pringle TH, Zahler AM, Haussler D. The human genome browser at UCSC. Genome Research. 2002;12:996-1006.

[125] BDNF brain derived neurotrophic factor [Homo sapiens (human)] | NCBI [Internet]. [cited 27 June 2022]; Available at: https://www.ncbi.nlm.nih.gov/gene/627

[126] Guarracino A, Pepe G, Ballesio F, Adinolfi M, Pietrosanto M, Sangiovanni E, Vitale I, Ausiello G, Helmer-Citterich M. BRIO: a web server for RNA sequence and structure motif scan. Nucleic Acids Research. 2021;49:67-71.

[127] Gruber AR, Lorenz R, Bernhart SH, Neuböck R, Hofacker IL. The vienna RNA websuite. Nucleic Acids Research. 2008;36:70-4.

[128] Zhang J, Kong L, Guo S, Bu M, Guo Q, Xiong Y, Zhu N, Qiu C, Yan X, Chen Q, Zhang H. hnRNPs and ELAVL1 cooperate with uORFs to inhibit protein translation. Nucleic Acids Research. 2017;45:2849-64.

[129] Solomon S, Xu Y, Wang B, David MD, Schubert P, Kennedy D, Schrader JW. Distinct Structural Features of Caprin-1 Mediate Its Interaction with G3BP-1 and Its Induction of Phosphorylation of Eukaryotic Translation InitiationFactor 2α, Entry to Cytoplasmic Stress Granules, and Selective Interaction with a Subset of mRNAs. Molecular and Cellular Biology. 2007;27:2324-42.

[130] Kearse MG and Wilusz JE. Non-AUG translation: a new start for protein synthesis in eukaryotes. Genes and Development. 2017;31:1717-31.

[131] Sample PJ, Wang B, Reid DW, Presnyak V, McFadyen IJ, Morris DR, Seelig G. Human 5′ UTR design and variant effect prediction from a massively parallel translation assay. Nature Biotechnology. 2019;37:803-9.

6 Appendix

Table A1- Forward and reverse primers used to generate desired *BDNF* 5′ UTR sequences by PCR.

Template	Desired Product	5′-3′ Forward primer	5′-3′ Reverse primer
BDNF v14 WT	*BDNF* v14 Δexon 2	AAGTCTGACGTCACGTCTC AGCAGCCTGGAGCTCCGGG	GGGGTCGTACACCTTGGAAG CCATCACTCTTCTCACCTGG TGGAACTCGGGGTCCACACA AAC
BDNF v11 WT	*BDNF* v11 WT ΔHuR-A + Caprin1 overlapping motifs	***BDNF*v11-uFwd** AAGTCTGACGTCACGTCTC AGTAAACCAATAGCCCCCA TG ***BDNF*v11-HuR-A+Caprin1-Fwd** TAGAGTGGGATGCAAAAAT AACCC	***BDNF*v11-uRev** GGGGTCGTACACCTTGGAAG CCATCACTCTTCTCACCTGG ***BDNF*v11-HuR-A+Caprin1-Rev** GGGTTATTTTTGCATCCCAC TCTATACTTAACTTCCCGCA CCTT
BDNF v11 WT	*BDNF* v11 WT ΔHuR-B motif	***BDNF*v11-uFwd** AAGTCTGACGTCACGTCTC AGTAAACCAATAGCCCCCA TG ***BDNF*v11-HuR-B-Fwd** ATGAGTGCACAAGGTTAAT CC	***BDNF*v11-uRev** GGGGTCGTACACCTTGGAAG CCATCACTCTTCTCACCTGG ***BDNF*v11-HuR-B-Rev** GATTAACCTTGTGCACTCAT CTGGTGGCTCCACACATCCA
BDNF v11 WT ΔHuR-A+Caprin1 motifs	*BDNF* v11 WT ΔHuR-A + Caprin1 + HuR-B motifs	***BDNF*v11-uFwd** AAGTCTGACGTCACGTCTC AGTAAACCAATAGCCCCCA TG ***BDNF*v11-HuR-B-Fwd** ATGAGTGCACAAGGTTAAT CC	***BDNF*v11-uRev** GGGGTCGTACACCTTGGAAG CCATCACTCTTCTCACCTGG ***BDNF*v11-HuR-B-Rev** GATTAACCTTGTGCACTCAT CTGGTGGCTCCACACATCCA
BDNF v11 exon 2 TTG	*BDNF* v11 exon 2 TTG ΔSegment 1	***BDNF*v11-uFwd** AAGTCTGACGTCACGTCTC AGTAAACCAATAGCCCCCA TG	***BDNF*v11-uRev** GGGGTCGTACACCTTGGAAG CCATCACTCTTCTCACCTGG

		Seg1Fwd ACAACTGGTTGTGTGGAGCCAC	**Seg1Rev** CTCCACACAACCAGTTGTCTTCCCGCACCTTCCTGCACTA
BDNF v11 exon 2 TTG	*BDNF* v11 exon 2 TTG ΔSegment 2	***BDNF*v11-uFwd** AAGTCTGACGTCACGTCTCAGTAAACCAATAGCCCCCATG **Seg2Fwd** ATCCTTGTTACTACTCAGATTGCT	***BDNF*v11-uRev** GGGGTCGTACACCTTGGAAGCCATCACTCTTCTCACCTGG **Seg2Rev** GCAATCTGAGTAGTAACAAGGATCCTTCGGGTTATTTTTGCAA
BDNF v11 exon 2 TTG	*BDNF* v11 exon 2 TTG ΔSegment 3	***BDNF*v11-uFwd** AAGTCTGACGTCACGTCTCAGTAAACCAATAGCCCCCATG **Seg3Fwd** CCACACTTGTTTTGGCGTCTAC	***BDNF*v11-uRev** GGGGTCGTACACCTTGGAAGCCATCACTCTTCTCACCTGG **Seg3Rev** TAGACGCCAAAACAAGTGTGGTAACCTTGTGCACTCAAGG
BDNF v11 exon 2 TTG	*BDNF* v11 exon 2 TTG ΔSegment 4	***BDNF*v11-uFwd** AAGTCTGACGTCACGTCTCAGTAAACCAATAGCCCCCATG **Seg4Fwd** CATCCCAGAAGAAGGGCTGTG	***BDNF*v11-uRev** GGGGTCGTACACCTTGGAAGCCATCACTCTTCTCACCTGG **Seg4Rev** CAGCCCTTCTTCTGGGATGACCTGCAACCCTTTCTGTAGA
BDNF v11 exon 2 TTG	*BDNF* v11 exon 2 TTG ΔSegment 5	***BDNF*v11-uFwd** AAGTCTGACGTCACGTCTCAGTAAACCAATAGCCCCCATG **Seg5Fwd** AACAAACTGATCCCTGAAATTGG	***BDNF*v11-uRev** GGGGTCGTACACCTTGGAAGCCATCACTCTTCTCACCTGG **Seg5Rev** ATTTCAGGGATCAGTTTGTTCACAGTCAAGCCAAACAGAA
BDNF v11 exon 2 TTG	*BDNF* v11 exon 2 TTG ΔSegment 6	***BDNF*v11-uFwd** AAGTCTGACGTCACGTCTCAGTAAACCAATAGCCCCCATG **Seg6Fwd** GGATGGTAATAAAGTCTCTTAGTGGT	***BDNF*v11-uRev** GGGGTCGTACACCTTGGAAGCCATCACTCTTCTCACCTGG **Seg6Rev** ACTAAGAGACTTTATTACCATCCAAATTCCACTGAAACGT

BDNF v11 exon 2 TTG	*BDNF* v11 exon 2 TTG ΔSegment 1a	***BDNF*v11-uFwd** AAGTCTGACGTCACGTCTCAGTAAACCAATAGCCCCCATG **Seg1aFwd** AAAAGAAATTATAGAGTGGGTT	***BDNF*v11-uRev** GGGGTCGTACACCTTGGAAGCCATCACTCTTCTCACCTGG **Seg1aRev** TTGCAACCCACTCTATAATTTCTTTTCTTCCCGCACCTTC
BDNF v11 exon 2 TTG	*BDNF* v11 exon 2 TTG ΔSegment 1b	***BDNF*v11-uFwd** AAGTCTGACGTCACGTCTCAGTAAACCAATAGCCCCCATG **Seg1bFwd** TTAAGTAATTATAGAGTGGGTTGCAAAAA	***BDNF*v11-uRev** GGGGTCGTACACCTTGGAAGCCATCACTCTTCTCACCTGG **Seg1bRev** GCAACCCACTCTATAATTACTTAACTTCCCGCACCTTCCTGC
BDNF v11 exon 2 TTG	*BDNF* v11 exon 2 TTG ΔSegment 1c	***BDNF*v11-uFwd** AAGTCTGACGTCACGTCTCAGTAAACCAATAGCCCCCATG **Seg1cFwd** TTAAGTAATTAAAAGAAATTTTGCAAAAATAACCCGAAGG	***BDNF*v11-uRev** GGGGTCGTACACCTTGGAAGCCATCACTCTTCTCACCTGG **Seg1cRev** CGGGTTATTTTTGCAAAATTTCTTTTAATTACTTAACTTCCCGCACCTTC

***Note- The remaining *BDNF* 5′ UTR sequences that were investigated were ordered directly.**